ADVANCES IN PHYSICS, 1978, VOL. 27, NO. 5, 747–798

Dispersive (non-Gaussian) transient transport in disordered solids

By G. PFISTER and H. SCHER
Xerox Webster Research Center,
Webster, New York 14580, U.S.A.

[Received 24 April 1978]

ABSTRACT

The experimental manifestations of dispersive (non-Gaussian) transient transport in disordered solids are discussed and compared with the predictions of theoretical treatments. The mathematical equivalence of the two theoretical approaches based on the formalisms of continuous-time random-walk (CTRW) and generalized multiple-trapping is demonstrated. Several transport mechanisms are discussed, viz. extended state motion with multiple trapping, hopping and trap-controlled hopping. Experimental studies on the chalcogenide glasses a-Se and a-As_2Se_3 are emphasized but results for organic solids and a-SiO_2 are included. There is independent evidence that transport occurs by a hopping process for the organic systems, but no such clear evidence exists for the inorganic solids. Nevertheless, on the basis of the temperature behaviour of the transit time dispersion and the values of parameters obtained from numerical analysis, we argue that hopping is also the microscopic transport mechanism in the inorganic solids.

For a-As_2Se_3 and a-SiO_2 the hopping time distribution function assumes the algebraic form $\psi(t) \sim t^{-(1+\alpha)}$ where $0 < \alpha < 1$ and $\alpha \sim$ const. For the organic systems and a-Se, more complicated time and temperature dependences of the distribution function are necessary to fit the data at all temperatures. In this context the observation of a transition from dispersive to non-dispersive transport as a function of increasing temperature in a-Se and poly-(*N*-vinylcarbazole) (PVK) is of particular interest. The subtle role played by local morphology in generating a transit time dispersion is demonstrated by comparing PVK and its brominated derivative 3Br–PVK.

A special section will be devoted to time-dependent electrical phenomena of metal semiconductor surfaces. That discussion will include a description of the experimental procedures necessary to identify the nature of contacts and their influence on the interpretation of steady-state conductivity data.

CONTENTS

§ 1. Introduction

A unifying feature of disordered solids is the broad distribution of event times that characterizes many of their time-dependent physical properties. This feature is independent of the detailed atomic or molecular structure of the solid and therefore gives rise to universal behaviour of a large number of disordered solids, whether organic or inorganic. Several examples are well known. The frequency dependence of the a.c. conductivity varies as ω^s where $s \lesssim 1$. The temperature dependence of the dielectric and elastic relaxation at the glass transition T_g exhibits the WLF temperature dependence

$$1/\tau = 1/\tau_0 \exp\left[C_1(T - T_g)/(C_2 + T - T_g)\right],$$

where, for most systems studied, the coefficients τ_0, C_1 and C_2 are approximately material-independent (see, for instance, McCrum *et al.* 1967). The low-temperature ($\lesssim 1$ K) acoustic and dielectric behaviour also shows some properties unique to the disordered state. The specific heat varies linearly with temperature, exceeding the Debye T^3 contribution by about a factor of 1000 (Zeller and Pohl 1971). This extra heat is attributed to the presence of another type of distribution, that of low energy excitations. The density of these excitation states is $\sim 10^{17}$ cm^{-3}, again independent of the material. Low-temperature acoustic attenuation is very similar in all disordered solids and the acoustic coupling constant in dielectric glasses is ~ 20 J cm^{-3}, which means that the elastic dipole moment associated with the low-energy excitation is approximately independent of the material (for a recent review, see Dransfeld and Hunklinger 1977). Similar behaviour has been reported for amorphous metals.

Recently there has been considerable interest in a transient time-dependent property that has been observed in time-of-flight experiments and is unique to the presence of disorder (Pfister and Scher 1977) (the disorder can be

generated by many types of trapping states in a crystalline material). It was noted that a sheet of net charges injected into the solid undergoes a significant broadening as it propagates through the bulk in the presence of an external field. In fact, due to the wide distribution of the statistical event times, the broadening can be so substantial that Gaussian statistics can no longer be applied. We are presented with the interesting situation that the distribution of event times extends into the time range characteristic of the experiment, viz. the time necessary for an appropriate portion of the injected carriers to complete their drift through the sample (transit time t_T).

The failure of Gaussian statistics to describe the dynamics of the propagating carrier packet in time-of-flight experiments introduces a number of novel physical phenomena which are being observed in an increasing number of disordered solids.

This review deals with the novel aspects of transient transport in disordered solids. Emphasis is on the properties of a-Se and a-As_2Se_3, but the essential observations for other disordered solids, in particular organic materials, are summarized. The review does not address physical properties other than transient (non-steady state) phenomena since steady-state properties of amorphous solids have been discussed in a number of recent review articles (Mott 1977, Owen and Spear 1977, Mort and Pai 1977). We start with a non-mathematical description of non-Gaussian transient transport (§ 2.1) before a more rigorous mathematical treatment is given (§ 2.2). Emphasis is on the general principles that govern non-Gaussian transport, which is demonstrated using the continuous-time random-walk (CTRW) formalism. Other mathematical treatments and computer simulations of non-Gaussian transport are then reviewed. In particular, the equivalence of a generalized multiple-trapping formalism (Noolandi 1977 b, Schmidlin 1977 a, b) and CTRW is outlined. The mathematical formalism is then applied to discuss three specific transport mechanisms : extended state transport, hopping and trap-controlled hopping.

In § 3.2 pertinent experimental results are surveyed and the general features of non-Gaussian transport are illustrated for transient hole transport in a-Se and a-As_2Se_3. A connection between transient and steady-state measurements necessitates a discussion of contact properties and transient dark injection (§ 3.3). Several additional examples for disordered solids exhibiting non-Gaussian transport are discussed in § 3.4.

In § 4 the mathematical description of transport mechanisms is compared with the experimental information. While the microscopic details underlying charge transport in the amorphous chalcogenides cannot be pinned down with certainty, it is argued that the holes in these materials propagate by a hopping process rather than in extended states. Similar transport mechanisms are proposed for the organic systems. For the latter materials, the experimental evidence for a specific transport mode is much more substantial, since the transport state can be controlled by sample preparation.

§ 2. Theoretical background

2.1. *Non-mathematical description of non-Gaussian transport*

Time-of-flight experiments on a-As_2Se_3 films demonstrate that holes, injected by a pulse of light from the sample surface, propagate through the bulk

in a manner that cannot be described by conventional Gaussian statistics (Scharfe 1970, Pfister 1974, Scher and Montroll 1975, Pfister and Scher 1977 a). That is, the dispersion σ of the carrier sheet and the mean displacement l from the illuminated surface do not obey the well-known relations $\sigma \propto t^{1/2}$ and $l \propto t$ which are expected from Gaussian statistics. The experimental transient hole current traces demonstrate a significant spreading of the hole packet as it propagates through the sample film. In fact, whereas for Gaussian statistics $\sigma/l \sim t^{-1/2}$, the observed current traces indicate that the spread σ and the mean displacement l feature the *same* time dependence, i.e. $\sigma/l = \text{const}$. These experimental results led to the recognition that the microscopic processes which control hole transport in a-As_2Se_3 must be characterized by a wide distribution of event times (Scher and Montroll 1975, Pfister and Scher 1977 a, b). Specifically, to obtain non-Gaussian behaviour, the event time distribution has to extend into the time range of the experimental observation determined by the transit time t_T which measures the transit of an appropriate fraction of the (fastest) injected carriers. Such broad distributions can easily be manifested in hopping transport where trivial fluctuations of the hopping distance and/or activation energy can introduce significant fluctuations in the nearest neighbour hopping time due to the strong localization of the charge carrier and the large activation energy typical for these low mobility solids (0·4–0·6 eV). Similarly, in the case of multiple trapping transport, broad release time distributions can be obtained for small fluctuations of mobility-limiting traps of sufficient depth. Scher and Montroll (SM) showed from first principles that in the non-Gaussian case the distribution function $\psi(t)$ which describes the probability for an event to happen at time t after the preceding event is a slowly decaying function of time.

For hole transport in a-As_2Se_3, the distribution function $\psi(t)$ can be approximated by the slowly varying power dependence

$$\psi(t) \sim t^{-(1+\alpha)},$$

where the disorder parameter α assumes a value between zero and unity. This distribution function sharply contrasts with the exponential time dependence

$$\psi(t) \sim \exp(-t/\tau),$$

which is associated with a single event time τ and is sufficient (but not necessary) to describe the Gaussian case. As will be discussed in following sections, for a-As_2Se_3 α is roughly constant, $\sim 0{\cdot}5$, for a wide range of experimental conditions (temperature, pressure, sample thickness, applied field). In contrast to this, a description of hole transport in a-Se requires a more complicated $\psi(t)$ which is temperature-dependent; only at low temperatures is the power time dependence approached (Noolandi 1977 a). The weak time dependence of $\psi(t)$ necessary to explain transient hole transport in a-As_2Se_3, and in a-Se at low temperatures, clearly reflects the fact that there is no characteristic time for the transport behaviour. The algebraic time dependence of $\psi(t)$ produces some novel behaviour of the transport properties, as a function of field, temperature, sample thickness and time, which can be checked by experiment (§ 3).

SM use the formalism of continuous-time random-walk (CTRW) to calculate the transient current observed in a time-of-flight experiment. For the special case of an algebraic $\psi(t)$, they are able to provide a complete mathematical description of the transport properties in terms of a single parameter α the

value of which depends upon the detailed microscopic transport process and has been calculated for the cases of hopping at fixed activation energy and extended state transport with multiple-trapping by a distribution of traps (see derivation and references in § 2.2).

Independent of the detailed transport mechanism, the general behaviour of the experimental observables can be qualitatively predicted once the concept of the broad event time distribution has been accepted. Indeed, although the mathematics of the non-Gaussian statistics describing the time-evolution of the carrier packet are not conventional, the final results are transparent and can be qualitatively described. Before proceeding to the detailed theoretical predictions, let us consider what qualitative features are to be expected for non-Gaussian transport.

We first recall that in the Gaussian case the time development of the injected carrier sheet can be described in terms of the mean displacement l from the illuminated surface and the dispersion σ which characterizes the spread of the charge sheet about the mean (fig. 1 (*a*)). The current induced by the drifting

Fig. 1 (*a*)

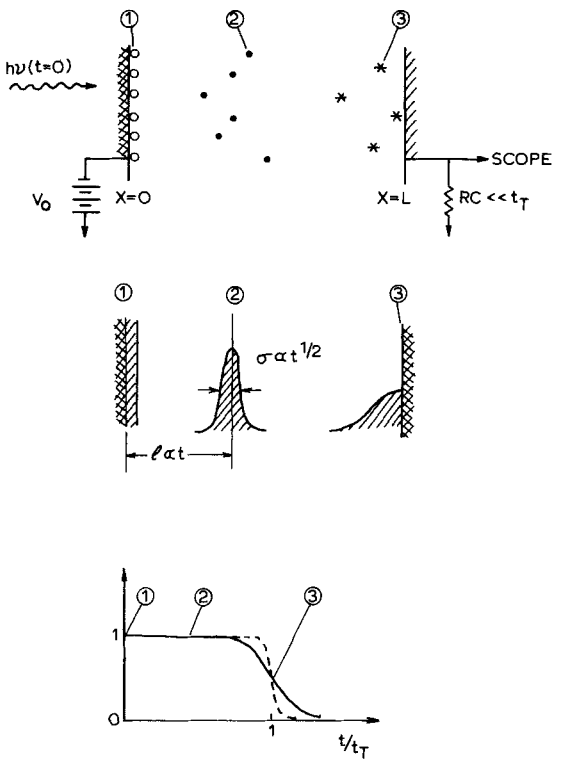

Schematic representation of carrier propagation under Gaussian conditions. Top : Position of representative carriers in the sample bulk at $t=0$ (○), $t<t_T$ (●) and $t\sim t_T$ (*). Middle : Charge distribution in sample bulk at $t=0$, $t<t_T$ and $t\sim t_T$. Bottom : Current pulse in external circuit induced by charge displacement. Units normalized to t_T and $i_T=i(t_T)$. Dashed line represents transient current for lower applied bias field, i.e. longer transit time.

Fig. 1 (*b*)

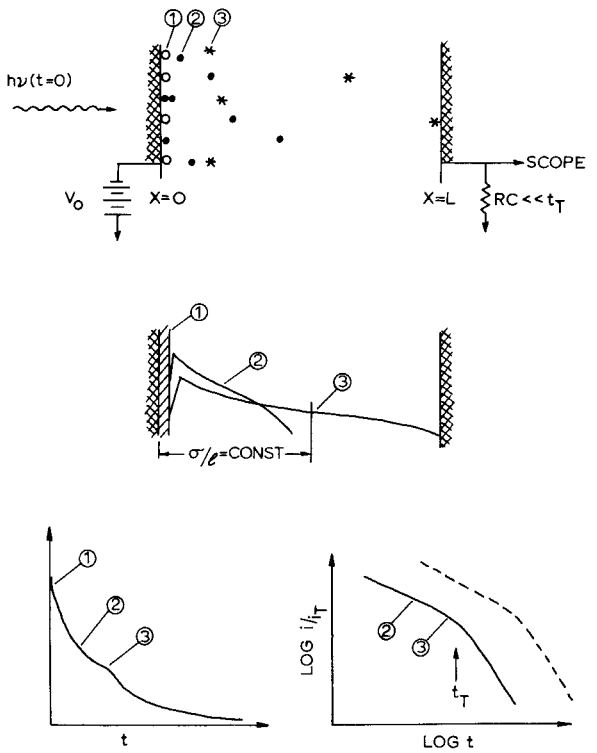

Schematic representation of carrier propagation under ideal non-Gaussian conditions. Top: Position of representative carriers in the sample bulk at $t=0$ (○), $t<t_T$ (●) and $t\sim t_T$ (*). Middle: Charge distribution in sample bulk at $t=0$, $t<t_T$ and $t\sim t_T$. Bottom: Current pulse in external circuit induced by charge displacement in linear units (left) and logarithmic units (right). Dashed line represents transient current for lower applied bias field, i.e. longer transit time.

charge sheet is $I=eq\mu_d E/L$ where μ_d is the drift mobility and q the number of injected carriers. If one neglects deep trapping of the carriers in transit, i.e. $\mu_d E\tau \gg L$, where τ is the deep trapping lifetime, the transient current remains constant, independent of the spreading σ about the mean l. When the leading edge of the carrier packet reaches the back electrode, the current begins to drop, and the width of the current decay is a measure of the dispersion σ at that time. Usually the time when the peak of the charge packet strikes the back electrode is identified with the transit time t_T. Hence, for a carrier packet spreading according to Gaussian statistics, $(\sigma/l)_{t_T} \propto t_T^{-1/2}$, i.e. the current pulse will sharpen with increasing transit time when plotted in units of t_T (by lowering the external field, for instance).

In the dispersive non-Gaussian case, the carrier packet is not expected to grow symmetrically about its mean position. Immediately after the occurrence of the carrier-producing light flash some carriers will rapidly move out of the generation region due to a rare succession of short event times. As time

evolves, an increasing number of carriers will suffer an event that can immobilize them for times of the order of the observation time, t_T. Under extreme non-Gaussian conditions, the distribution of the carrier packet grows asymmetrically featuring a leading edge penetrating deep into the bulk, while the maximum of the charge density moves only slowly out of the generation region (fig. 1 (*b*)). For such asymmetric carrier propagation, the spread and the mean position have the same time dependence, hence $\sigma/l = \text{const}$. Thus the shape of the transient current is independent of the transit time when plotted in units of t_T, a feature which has been termed ' universality of the current shape '.

The mean drift velocity v_d of the propagating carrier packet must decrease with time since, for sufficiently broad event time distributions, the number of carriers immobilized for a time of the order of t_T must grow. With v_d time dependent, the transit time $t_T = L/v_d$ must increase faster than proportional to the sample thickness, implying a thickness-dependent drift mobility $\mu_d = L/t_T E$. This feature, of course, is in sharp contrast with the Gaussian case where the drift mobility is a well-defined intrinsic quantity.

The general result of the CTRW obtained for an algebraic distribution function $\psi(t) \propto t^{-(1+\alpha)}$ is summarized in the following equations (Scher and Montroll 1975)

$$I(t) \sim \begin{cases} t^{-(1-\alpha)}, & t < t_T \\ t^{-(1+\alpha)}, & t > t_T \end{cases} \tag{1}$$

$$t_T \sim \left(\frac{L}{l(E)}\right)^{1/\alpha} \exp(\Delta/kT), \tag{2}$$

where $0 < \alpha < 1$ is defined by the time dependence of the distribution function. Following eqn. (1), the rate of current decay increases at a characteristic time t_T (' transit time '). At this time the rate of carrier loss at the substrate electrode begins to dominate the rate of temporary carrier immobilization in the bulk of the sample. Thus, t_T approximately characterizes the time when the leading edge of the carrier packet reaches the absorbing substrate. Equation (2) predicts the expected superlinear relationship between sample thickness and transit time. Furthermore, the shape of the transient current $I(t)$ and the field and thickness dependence of the transit time t_T are correlated via the disorder parameter α. The smaller α, the stronger the (E/L)-dependence of t_T and the more dispersive the shape $I(t)$. At constant temperature, α is roughly constant, hence the current shape displays the scaling property $\sigma/l \sim \text{const}$. Finally, the sum of the power exponents describing the time dependence of $I(t)$ at times shorter and longer than t_T equals -2 and is therefore independent of the actual disorder and underlying transport mechanism.

Equations (1) and (2) strictly apply to dispersive transport which can be characterized by an algebraic time dependence of the distribution function $\psi(t)$. More complicated $\psi(t)$ expressions may be necessary to explain the experimental data over broad experimental ranges. Hole transport in a-Se constitutes an example where a complete transition from non-dispersive Gaussian to dispersive non-Gaussian transport can be observed as a function of decreasing temperature (Pfister 1976). In addition to non-algebraic distribution functions, deviations from the current shapes given by eqn. (1) are expected if the evolution of the spreading of the propagating carrier packet

is distorted by non-uniform fields due to space-charge and surface trapping. The latter case has recently been discussed in connection with corresponding observations made for hole transport in a-As_2Se_3 (Pfister and Scher 1977 a). For the generation of the data presented in § 3, care has been taken to avoid distortion of the current shape. For a-Se and a-As_2Se_3 this can be approximately achieved by low levels of carrier injection ($\ll CV$), proper choice of the electrode material, extensive dark resting and adjusted time delay between the application of the bias field and the flash occurrence. Increasing the complexity of $\psi(t)$ inevitably leads to a larger number of independent parameters which can be extracted from the experimental current traces only by elaborate computer fits. For the discussion of the experimental results in § 3 we restrict ourselves to a comparison with the theoretical predictions based upon the algebraic distribution function, i.e. eqns. (1) and (2) which contain all the principal features underlying dispersive transient transport.

The remainder of § 2 describes the mathematical formalisms used to explain dispersive transport. In particular, the formalism of continuous-time random-walk and the equivalence between the CTRW and the more conventional generalized multiple-trap formalism are emphasized. The CTRW is then applied to discuss several transport mechanisms, viz. multiple-trapping, trap-controlled hopping and conventional hopping.

2.2. *Mathematical formalism of CTRW on a lattice*

2.2.1. *Introduction*

In a system composed of a random distribution of molecular sites, the displacement between neighbouring molecules ρ as well as their energy level difference Δ varies from site to site. Although the systems considered here are homogeneous, i.e. the average molecular concentration and average energy difference are independent of the spatial variables ($\mathbf{r}$), the degree of this site-to-site variation is crucial for the physical properties we are investigating. These random variations have a large effect on the spread of transition rates between the molecules. The transition rates themselves in a real physical system can depend on variables other than ρ and Δ, e.g. on the relative angular configuration of the molecules (Slowik 1977). However complicated the form of the transition rates and the details of the molecular charge transfer, it is assumed that these rates depend sensitively on a number of parameters that are statistically distributed. Thus, even rather mild variations of some system parameters ' map ' onto a broad distribution of transition rates. This mapping is not unique. A number of different parameter dispersions can produce very similar transition rate distributions. There can be gross distinctions, such as differences in temperature dependence, between various microscopic mechanisms. This will be discussed in the following sections. The point emphasized here is that a model based on the distribution of rates as the primary input is the important level of description for the time-dependent phenomena in these disordered systems.

One way to sample these rates is to observe a carrier move along some path. The carrier encounters a series of nearest-neighbour hops or capture and release from traps. Most of these time events will be short and a few will be long on the time scale of observation.

One can ' fold ' this distribution of time events into a single probability distribution function $\psi(t)$ (as introduced in the preceding section) to leave a given site. As the $\psi(t)$ represents a properly weighted statistical sampling of the entire distribution of fluctuating rates over the time history of a path, it is not surprising that a transport model using $\psi(t)$ will be non-Markoffian. A system is Markoffian if the present value of a set of parameters, defining the system, determines the future characterization of the system. It is non-Markoffian in a very specific way. The only additional information needed to specify the state of a system, besides the probability of occupancy of the sites at time t, is the time of arrival at each site. No knowledge of previous states of the system for times $t' < t$ is needed. This is in contrast to a recent discussion of the non-Markoffian properties of this transport model (Pollak 1977). In fact this process is known technically as semi-Markoffian (Pyke 1961).

The model is a continuous-time random-walk (CTRW) on a lattice with $\psi(t)$ determining the random times to leave each site, and $p(\mathbf{s})$ the spatial displacement probability at each step. The electric field $\mathbf{E}$ dependence, which causes a spatial asymmetry, is included in $p(\mathbf{s})$. The lattice parameter a_0 is the mean hopping distance or mean distance between trapping events.

In order to further motivate this model, we can consider a system composed of periodically reproduced large cells ; each cell containing n randomly placed sites, where $n \gg 1$. One can solve such a model exactly ; however, the $\psi(t)$ becomes a $n \times n$ matrix $\psi_{ij}(t)$. The picture of a carrier leaving a cell at various random times is now seen simply as the different ways it hops out of the cell from each of the n sites. While this is more graphic, the actual computational details would be very involved. Satisfactory results would most assuredly be obtained by introducing an effective $\psi_{\text{eff}}(t)$ with a cell parameter a_0 that would reproduce the use of $\psi_{ij}(t)$ with a larger cell size.

We now consider the computation of a CTRW with a more general $\psi(\mathbf{s}, t)$ and specialize to the factorization $p(\mathbf{s})\psi(t)$ below. The $p(\mathbf{s})$ determines the spatial asymmetry of the carrier displacement, e.g. it contains the electric field dependence.

2.2.2. *The mathematical model*

The basic quantity in a CTRW, with time as a continuous variable, is $P(\mathbf{s}, t|\mathbf{s}_0)$, the probability of the carrier being *found* at $\mathbf{s}$ at time t if it started from $\mathbf{s}_0$ at $t=0$. One must allow for the possibility that the carrier could arrive at $\mathbf{s}$ at an earlier time $\tau < t$ and remain at $\mathbf{s}$ for at least the time interval $t-\tau$. This is done by introducing an auxiliary function : let $R_n(s, t)\Delta t$ be the probability for a carrier to just arrive at $\mathbf{s}$ between t and $t+\Delta t$ in n steps, if it started at $t=0^+$ and $\mathbf{s}_0$ (we will suppress the $\mathbf{s}_0$ dependence for brevity) where

$$\mathbf{s} = s_1\hat{a}_1 + s_2\hat{a}_2 + s_3\hat{a}_3, \tag{3}$$

and s_i is equal to an integer, $\hat{a}_i$, the unit primitive translation vectors of the lattice. The random walks (RW) are restricted to be on infinite lattices or on finite lattices (N^3 distinct points) with periodic boundary conditions.

The central aspect of any RW is the step-by-step generation of the probability to arrive at a given site. The probability of reaching the site s in $n+1$

steps is simply related to the previous one in n steps at some other site

$$R_{n+1}(\mathbf{s}, t) = \sum_{s'} \int_0^t d\tau\, \psi(\mathbf{s}-\mathbf{s}', t-\tau) R_n(\mathbf{s}', \tau). \tag{4}$$

where $\psi(\mathbf{s}, t)\Delta t$ is the probability that successive steps occur between t and $t+\Delta t$ and the displacement is $\mathbf{s}$. The R_n function is thus observed to be the n-fold convolution of factors, i.e. it is a sum of the probabilities of all the paths, each with cumulative n random times adding up to time t. The relation between R and P occurs at the last step as will be shown below.

The function of immediate interest is

$$R(\mathbf{s}, t) \equiv \sum_{n=0}^{\infty} R_n(\mathbf{s}, t), \tag{5}$$

the probability per unit time to reach s in time t, independent of the number of steps to get to s. Thus, summing eqn. (4) over n and inserting the initial condition :

$$R_0(\mathbf{s}, t) = \delta_{\mathbf{s},0}\delta(t-0^+), \tag{6}$$

one obtains

$$R(\mathbf{s}, t) - \sum_{s'} \int_0^t d\tau\, \psi(\mathbf{s}-\mathbf{s}', t-\tau) R(\mathbf{s}', \tau) = \delta_{\mathbf{s},0}\delta(t-0^+). \tag{7}$$

The form of eqn. (7) lends itself to solution by transform techniques, which reduces eqn. (7) to an algebraic one.

One takes the Laplace transform of eqn. (7) to obtain :

$$\tilde{R}(\mathbf{s}, u) - \sum_{s'} \tilde{\psi}(\mathbf{s}-\mathbf{s}', u)\tilde{R}(\mathbf{s}', u) = \delta_{\mathbf{s},0}, \tag{8}$$

where

$$\tilde{\psi}(\mathbf{s}, u) = \int_0^{\infty} dt \exp(-ut)\, \psi(\mathbf{s}, t). \tag{9}$$

The solution of eqn. (8) is accomplished with the use of Fourier transforms ($k_i = 2\pi m_i/a_i N$, m_i integer) :

$$U(\mathbf{k}, u) = \sum_{s} \tilde{R}(\mathbf{s}, u) \exp(-i\mathbf{k} \cdot \mathbf{s}), \tag{10}$$

with the result :

$$\tilde{R}(\mathbf{s}, u) = N^{-3} \sum_{k} \frac{\exp(i\mathbf{k} \cdot \mathbf{s})}{1-\Lambda(\mathbf{k}, u)}, \tag{11}$$

where

$$\Lambda(\mathbf{k}, u) = \sum_{s} \tilde{\psi}(\mathbf{s}, u) \exp(-i\mathbf{k} \cdot \mathbf{s}), \tag{12}$$

which can be called the generalized structure function of the CTRW.

The final part of the solution involves the relation between $P(\mathbf{s}, t)$ and $R(\mathbf{s}, \tau)$, $\tau < t$:

$$P(\mathbf{s}, t) = \int_0^t R(\mathbf{s}, \tau)\Phi(t-\tau)\, d\tau, \tag{13}$$

where $\Phi(t)$ is the probability that the walker remains fixed in the time interval $[0, t]$:

$$\Phi(t) = 1 - \int_0^t \psi(\tau)\, d\tau, \tag{14}$$

with

$$\psi(t) \equiv \sum_{s} \psi(\mathbf{s}, t). \tag{15}$$

Taking the Laplace transform of eqn. (13), we obtain a simple final expression :

$$\tilde{P}(\mathbf{s}, u) = \tilde{R}(\mathbf{s}, u)[1 - \tilde{\psi}(u)]/u, \tag{16}$$

where $\tilde{R}(\mathbf{s}, u)$ is given in eqn. (11).

Hence, one has obtained the Laplace transform of $P(\mathbf{s}, t)$, our basic propagator, as a function of $\Lambda(k, u)$, the transform of $\psi(s, t)$, the single distribution function ($\tilde{\psi}(u) \equiv \Lambda(0, u)$). To calculate the current $I(t)$ in a transient photoconductivity measurement, one must take the inverse Laplace transform of eqn. (16) and obtain $P(\mathbf{s}, t)$. In this latter case, one cannot evaluate $\mathscr{L}^{-1}P(\mathbf{s}, u)$ without specifying a definite $\psi(\mathbf{s}, t)$. It is at this point that one uses a simplified expression for $\psi(\mathbf{s}, t)$, namely

$$\psi(\mathbf{s}, t) = p(\mathbf{s})\psi(t), \tag{17}$$

where $p(\mathbf{s})$ describes the spatial asymmetry in the step displacement. To complete the calculation of $I(t)$, one must include the effects on $P(\mathbf{s}, t)$ of the absorbing boundary (Montroll and Scher 1973) and then equate $I(t)$ to the time derivative of the spatial mean $\langle \mathbf{s} \rangle$ of $P(\mathbf{s}, t)$. The results of that calculation are given in eqns. (1) and (2).

2.3. *Comparison with generalized multiple-trapping formalisms*

Both Noolandi (1977 b) and Schmidlin (1977 a, b) have made a comparison between the CTRW and multiple trapping. Their treatments differ in some details of interpretation. We have chosen to follow the discussion by Noolandi (1977 b) as his interpretation follows more closely the one discussed by ourselves (Pfister and Scher 1977 a).

In a multiple-trapping problem one usually solves the following set of linear transport equations :

$$\frac{\partial p}{\partial t} = g(\mathbf{r}, t) - \nabla \cdot \mathbf{f}(\mathbf{r}, t), \tag{18}$$

$$\rho(\mathbf{r}, t) = p(\mathbf{r}, t) + \sum_{i} p_i(\mathbf{r}, t), \tag{19}$$

$$\frac{\partial p_i(\mathbf{r}, t)}{\partial t} = p(\mathbf{r}, t)\omega_i - p_i(\mathbf{r}, t)W_i, \tag{20}$$

where $g(\mathbf{r}, t)$ is the local photogeneration rate, and f is the flux of mobile carriers which we can relate to the concentration of mobile carriers $p(\mathbf{r}, t)$, $\mathbf{f} = \mu \mathbf{E} p$, where μ is the mobility of the carriers. The concentration of carriers in the ith trap is $p_i(\mathbf{r}, t)$. The total concentration of carriers is $\rho(\mathbf{x}, t)$, defined by eqn. (19). The summation in eqn. (19) extends over all the different kinds of traps in the material. Each trap is characterized by a capture rate, ω_i, and a release rate, W_i. The trap parameters are assumed to be independent of $\mathbf{r}$, corresponding to a homogeneous trap distribution.

Equation (18) may then be written

$$\frac{\partial \rho}{\partial t} = g - \mu \mathbf{E} \cdot \nabla p. \tag{21}$$

In order to derive an equation for the total charge concentration, $\rho(\mathbf{x}, t)$, from eqn. (21), it is necessary to obtain a relation between $p(\mathbf{x}, t)$ and $\rho(\mathbf{x}, t)$. This can be done easily using eqn. (20) and introducing the Laplace transform (L.T.),

$$\tilde{p}(\mathbf{r}, u) = \int_0^\infty \exp(-ut)\, p(\mathbf{r}, t)\, dt, \tag{22}$$

giving

$$u\tilde{p}_i = \tilde{p}\omega_i - \tilde{p}_i W_i, \tag{23}$$

where we have assumed $p_i(\mathbf{r}, 0) = 0$. Using eqn. (23), we get immediately

$$\tilde{p} = \tilde{Q}\tilde{\rho}, \tag{24}$$

where

$$\tilde{Q} = \left\{1 + \sum_i \frac{\omega_i}{u + W_i}\right\}^{-1}. \tag{25}$$

According to the convolution theorem, the inverse transform of eqn. (24) is

$$p(\mathbf{r}, t) = \int_0^t Q(t-t')\rho(\mathbf{r}, t')\, dt', \tag{26}$$

and using this result in eqn. (21) gives

$$\frac{\partial \rho}{\partial t} = g - \mu E \int_0^t Q(t-t') \frac{\partial \rho(\mathbf{r}, t')}{\partial x}\, dt', \tag{27}$$

where the electric field is in the x direction.

It was necessary to derive an equation involving only the total charge concentration because now a direct comparison can be made with the equation governing the time dependence of $P(\mathbf{s}, t)$ in the CTRW. The total charge concentration is proportional to $P(\mathbf{s}, t)$. One uses the relation between $\tilde{R}(\tilde{s}, u)$ and $\tilde{P}(\tilde{s}, u)$ in eqn. (16) and inserts it into eqn. (8) which can be algebraically rearranged to yield

$$\frac{dP}{dt}(\mathbf{s}, t) = \int_0^t \phi(t-x)\Sigma[p(\mathbf{s}-\mathbf{s}')P(\mathbf{s}', x) - p(\mathbf{s}'-\mathbf{s})P(\mathbf{s}, x)]\, dx, \tag{28}$$

where

$$\tilde{\phi}(u) = u\tilde{\psi}(u)/[1-\tilde{\psi}(u)]. \tag{29}$$

One recognizes eqn. (28) as a generalized master equation with a relaxation function $\phi(t)$. An exponential $\psi(t) = W \exp(-Wt)$ yields $\phi(t) = 2W\delta(t)$, so that eqn. (28) reduces to an ordinary master equation which is local in time. A non-exponential $\psi(t)$, i.e. a distribution of rates W, leads to the non-local dependence on time exhibited by the generalized master equation.

One now sees the physical basis for the non-local time dependence in the multiple-trapping case. The free carrier concentration $p(\mathbf{s}, t)$ at time t has contributions from trapped charge which has been immobilized at an earlier time and subsequently released. If $\tilde{Q}(u)$ is weakly dependent on u, then $p(\mathbf{s}, t) \propto \rho(\mathbf{s}, t)$. This will occur if $u \ll W_i$ or $t \gg W_i^{-1}$. Thus if the time of interest is large compared to all the release times, the multiple-trap case will reduce to a local time dependence. If there is only one trap $i = 1$ then $t \gg W_1^{-1}$, otherwise there would be no *multiple* trapping. Hence, again we see that the

non-locality in time is related to a distribution of rates. In the trapping case it is a spread in the release rates W_i and the spread must extend over the time range of observation.

One more step is now needed to show the equivalence between the multiple trapping and the CTRW with an appropriate choice of $\psi(t)$. The form of the kinetic equations for the trapping case assume $\mathbf{r}$ to be a continuous variable, while the CTRW takes place on a discrete lattice. We, therefore, take the continuum limit of the generalized master equation and, neglecting diffusion, has been shown (Leal Ferreira 1977) to be

$$\frac{\partial \rho}{\partial t} = g - a_0 \Delta \int_0^t \phi(t-t') \frac{\partial \rho(x, t')}{\partial x} \, dt', \tag{30}$$

where a_0 is the lattice cell constant, and Δ is the asymmetry factor in the transition probability between cells caused by the electric field. The generation term has been included explicitly in eqn. (30). Equating the transforms of eqns. (28) and (30) (with $P = \rho$) gives

$$\tilde{\phi} = (\mu E / a_0 \Delta) \tilde{Q}, \tag{31}$$

and the relation between $\tilde{\phi}$ and $\tilde{\psi}$ in eqn. (29) leads to

$$\tilde{\psi} = (1 + u\tau \tilde{Q}^{-1})^{-1}, \tag{32}$$

where $\tau = (a_0 \Delta / \mu E)$ for convenience. Using eqn. (32), $\psi(t)$ can be calculated in terms of the trap parameters $\{\omega_i, W_i\}$, provided the quantity τ is defined independently.

2.4. *Transport mechanisms*

2.4.1. *Multiple trapping*

The formal equivalence between multiple trapping and the CTRW model has been demonstrated. Another, and perhaps, more physically transparent approach to the connection between trapping and the CTRW can be obtained by avoiding the continuum limit of the generalized master equation. Instead one makes the multiple-trap model discrete in the spatial variable. In fact, conventional multiple trapping, into various localized states, of a carrier moving in a band state is the simplest transport mode to understand, as the important stochastic variable, the release rate, W_i, is a single site quantity. The carrier moves an average distance $\mu\tau E$ before it is trapped in a particular level with a probability ξ_i. Thus, the lattice constant in the direction of the field a_0 is set equal to $\mu\tau E$ and $\psi(t)$ is simply a weighted sum of the probability per unit time to be released from one of the levels to the band,

$$\psi(t) = \sum_i \xi_i W_i \exp(-W_i t). \tag{33}$$

One can cast eqn. (33) into spectral form

$$\psi(t) = \int_0^\infty dW \, p(W) W \exp(-Wt), \tag{34}$$

where

$$p(W) = \sum_i \xi_i \delta(W - W_i), \tag{35}$$

is an *effective* spectrum of release rates. The term ' effective ' is used to indicate that each W_i in $p(W)$ is weighted by ξ_i, the probability the carrier encounters the ith level.

The $\tilde{\psi}(u)$ produced by the two approaches, (1) taking the continuum limit of the CTRW and (2) reducing the multiple-trapping problem to a discrete lattice case can now be shown to be the same in the asymptotic limit of many trapping events. From eqns. (32), (25) we have

$$\tilde{\psi}(u)=\left[1+u\tau+u\tau\sum_i\frac{\omega_i}{u+W_i}\right]^{-1}. \tag{36}$$

If we expand in powers of $u\tau$ and choose

$$\tau=\sum_i\omega_i, \tag{37}$$

we obtain a result equal to the L.T. of eqn. (33). Thus in the small $u\tau$ or $t\gg\tau$ limit the approaches are the same (in fact if one is not in that limit, *multiple* trapping makes no sense). The sum over i in eqn. (35) can now be converted into an integral over all the variables characterizing the capture probability and release rate. A particularly simple example will illustrate the main point :

$$p(W)=\int_0^\infty d\epsilon\, g(\epsilon)\delta(W-W(\epsilon))\xi(\epsilon), \tag{38}$$

where

$$g(\epsilon)=\begin{cases}0, & \epsilon<\epsilon_{\mathrm{m}}\\ N\exp\left[-(\epsilon-\epsilon_{\mathrm{m}})/kT_0\right], & \epsilon>\epsilon_{\mathrm{m}}\end{cases} \tag{39}$$

and

$$W(\epsilon)=\nu\exp\left(-\epsilon/kT\right). \tag{40}$$

The capture probability is assumed to be a slowly varying function of ϵ. Using eqns. (38)–(40) we obtain

$$p(W)=\begin{cases}0, & W>\nu_{\mathrm{T}}\\ \dfrac{NkT}{\nu}\exp\left(\dfrac{\epsilon_{\mathrm{m}}}{kT_0}\right)\left(\dfrac{W}{\nu}\right)^{(T/T_0)-1}\xi[kT\ln(\nu/W)], & W<\nu_{\mathrm{T}}\end{cases} \tag{41}$$

with $\nu_{\mathrm{T}}\equiv\nu\exp\left(-\epsilon_{\mathrm{m}}/kT\right)$. Note that, aside from logarithmic terms,

$$p(W)\propto W^{\alpha-1},\quad \alpha=T/T_0. \tag{42}$$

A $p(W)$ of the form of eqn. (42) leads to a $\psi(t)\sim t^{-1-\alpha}$ and therefore a multiple-trap mechanism with a $g(\epsilon)$ as in eqn. (39) can generate dispersive transport. An important point is that for this mechanism the α, as in eqn. (42), is *temperature dependent.* This T-dependent property persists with even more elaborate trapping models, provided $g(\epsilon)$ falls off sufficiently fast with $\epsilon>\epsilon_{\mathrm{m}}$, and is related to the fact that the spread in W is caused by a variation in trap depth ϵ.

This property is physically obvious because the carriers having transit times appearing in the tail of $I(t)$ must have experienced deeper traps than the carriers traversing the sample earlier. Hence the relative change of ' tail ' transit times with temperature is more rapid and thus changes the shape of $I(t)$.

One could have a trapping model where the spread in W is caused by a change in ν (eqn. (40)). However, the physical interpretation of a spectrum of ν corresponding to, e.g. one trap depth ϵ leads more naturally into a hopping model. This consideration leads to the larger question of whether the set of numbers $\{\xi_i, W_i\}$ in eqn. (33), defining the $\psi(t)$, have the specific physical meaning of capture and release parameters from a set of isolated trap states or does $\{\xi_i, W_i\}$ generate a particularly convenient mathematical basis to represent a $\psi(t)$? In other words, the $\psi(t)$ could correspond to a hopping motion and be represented by a judicious set of $\{\xi_i, W_i\}$ parameters. The $\psi(t)$ generated by Noolandi using eqn. (33) could have meaning independent of the parameters he used to fit a-Se data (Noolandi 1977 a). The form of $\psi(t)$ in eqn. (33) facilitates the computation of the pertinent inverse Laplace transforms in the CTRW, e.g. the spatial transforms $\gamma(k, t)$ of the propagator of the carrier packet, is determined by a set of discrete singularities of the integrand. One can thus rapidly generate a packet motion and the current corresponding to a general $\psi(t)$ represented by the ' basis set ' in eqn. (33).

If one uses a density of states with a finite width (i.e. a maximum trap energy), one could generate a spectrum of rates

$$p(W) = cW^{\alpha-1} \exp(-W_l/W), \tag{43}$$

which gives rise to a

$$\psi(t) = 2c(W_l/t)^{(\alpha+1)/2} K_{\alpha+1}[2(W_l t)^{1/2}], \tag{44}$$

where W_l is a minimum release rate which corresponds to the largest trap energy Δ_l and $K_\nu(x)$ is the modified Hankel Function. Now if the density of states is peaked around an energy Δ, the transit time could vary as $t_T \propto \exp(\Delta/kT)$ and $t_T W_l$ can increase with increasing T. Using eqn. (44) one can show that for $W_l t_T \ll 1$ one has dispersive transport and for $W_l t_T \gg 1$ non-dispersive or Gaussian transport. In addition, if there is a temperature-independent contribution to α, e.g. an energy dependence of ν, the $\psi(t)$ generated by the $p(W)$ in eqn. (43) can describe a Gaussian to non-Gaussian transition with decreasing temperature, with a weakly T-dependent α, and *no change* in the activation energy at the transition. It is important to point out that the $\psi(t)$ in eqn. (44) has an algebraic form only for $W_l t \ll 1$. The SM theory is not synonymous with the use of a $\psi(t)$ of an algebraic form. It should be emphasized that the form of $p(W)$ in eqn. (43) generates a $\psi(t)$ that serves as a model for a Gaussian to non-Gaussian transition. A different model for $\psi(t)$ based on the assumption of three traps has been used to fit the Gaussian to non-Gaussian transition in a-Se (Noolandi 1977 a).

2.4.2. *Hopping*

Time-dependent hopping among a random distribution of sites is a difficult but exciting theoretical problem. In modelling this problem with a CTRW on a lattice we rely on the ergodic nature of the transport process. The carrier in transversing the disordered medium samples a wide variety of environments (as discussed above). The distribution of hopping times, due to the variation in site separations and site energy fluctuations, over the entire medium is folded into the hopping time distribution to leave a single site, $\psi(t)$. Let us define the probability $Q(\mathbf{s}_0, t)$ for a carrier to stay on a site $\mathbf{s}_0$ in the disordered

solid. The $Q(\mathbf{s}_0, t)$ decays in time due to many *parallel* channels to leave the site

$$-\frac{dQ}{dt}(\mathbf{s}_0, t) = Q(\mathbf{s}_0, t) \sum_i W(\mathbf{s}_i - \mathbf{s}_0, \epsilon_i - \epsilon_0), \tag{45}$$

where $W(\mathbf{r}, \epsilon)$ is the transition rate to a site displaced by $\mathbf{r}$ and with a change of site energy ϵ. We calculate the configuration average of $Q(\mathbf{s}_0, t)$ and express it in spectral form,

$$\ln \Phi(t) \equiv \ln \langle Q(\mathbf{s}_0, t) \rangle = -\int_0^\infty dW\, [1 - \exp(-Wt)] p(W), \tag{46}$$

where

$$p(W) = \int d\epsilon\, d^3r\, g(\epsilon) \rho(\mathbf{r}) \delta[W - W(\mathbf{r}, \epsilon)], \tag{47}$$

$\rho(\mathbf{r}) d^3r$ is the probability a site is located in a volume d^3r centred about $\mathbf{r}$ and $g(\epsilon)$ is the probability density of changing the site energy by ϵ. $p(W)$ is a spectrum of rates and from the definition

$$\psi(t) = -\frac{d\Phi(t)}{dt}, \tag{48}$$

one has

$$\psi(t) = \int dW\, W p(W) \exp(-Wt)\, \Phi(t). \tag{49}$$

Thus, for a hopping problem the spectral form of $\psi(t)$ is *different* from eqn. (34) for the multiple-trap case. The difference lies in the fact that for the trapping problem one can assume a *supposition* of independent release rates (weighted by the probability of the carrier being in the level) because there is only one way to leave each state. In the hopping problem, the carrier can leave the state via *parallel* channels, therefore, the weighting of a specific 'release' rate $W \exp(-Wt)$ must include the probability of whether the carrier is still in the state ($\Phi(t)$). Hence, the physical interpretation of $\{\xi_i, W_i\}$ in eqn. (33) for a $\psi(t)$ *applied to a hopping problem* could be significantly modified.

One can calculate $\psi(t)$ for general $g(\epsilon)$ and $\rho(\mathbf{r})$. If we assume a spatially random site distribution, $\rho(\mathbf{r}) = N$, the site density, then one obtains,

$$\alpha = \frac{4\pi}{3} N R_0^3 \left[(\ln \tau)^2 - \frac{3\bar{\epsilon}}{kT} \ln \tau + \frac{3\bar{\epsilon}^2}{(kT)^2} \right], \tag{50}$$

where $\tau \equiv W_0 \exp(-\epsilon_0/kT)t$, and $\bar{\epsilon}$, $\bar{\epsilon}^2$ are the first and second moments of $g(\epsilon)$ measured with respect to ϵ_0, the peak position of $g(\epsilon)$.

One can also include percolation effects in $\psi(t)$ by introducing a spatial cut-off in $\rho(\mathbf{r})$.

2.4.3. *Trap-controlled hopping*

As discussed above, in general, one can have a carrier hopping through a material and experiencing fluctuations in the energy level of the localized site, as well as the dispersion in intersite separation. The fluctuation in energy levels will tend to increase the dispersion in hopping times and add temperature dependence to the effective α, as shown in the multiple-trap case above. If the carrier is interacting with hopping sites corresponding to distinct sets of energy levels, then the fluctuations can be discrete, as opposed to disorder-induced

energy fluctuations in, e.g. impurity hopping conduction in semiconductors (Scher and Lax 1973). For definiteness, we will consider two sets of states, and we will designate the sites as h and t, where the density N_h is much larger than N_t. The carrier can hop from h to h with an activation energy Δ_h and from t to h with Δ_t. If $\Delta_t > \Delta_h$ then the *typical* hop time τ_t from t to h is much greater than the typical hop time τ_h from h to h. We call this situation trap-controlled hopping because there is a *discrete* separation between the spectrum of τ_h and τ_t. Although there are two activation energies in this hopping case, the transit time activation can range from Δ_h to Δ_t depending on the relative densities N_h/N_t. For $N_h \gg N_t$ there will be a large number of hopping paths that do not pass through a t site ; hence, most of the fastest carriers (which determine t_T) will not encounter a hop with Δ_t. As N_t increases, the number of paths that do not contain a t site decreases and the activation energy Δ of t_T tends to Δ_t.

To recap, in hopping the nature of the dispersion, as exemplified by α, and the displacement between events are correlated. In trap-controlled hopping this correlation is not operative. One can independently vary the number of events and the dispersion of event times. *The rate-limiting steps are the release times from a set of isolated trapping sites (density N_t), while the dispersion of the release times is determined by the local distribution of hopping sites (density N_h) around the trap, as well as any fluctuation in the trap energy.*

The $\psi(t)$ for trap-controlled hopping is calculated in the same way it is for hopping (§ 2.4.2). However, the mean spatial displacement is determined by the both N_h, N_t and the electric field E.

If $E=0$, the carrier diffuses away isotropically and the mean spatial displacement between trapping events is $\sim N_t^{-1/3}$, or the mean volume swept out by the carrier is N_t^{-1}. For finite E, the mean volume is still $\sim N_t^{-1}$; however, the spatial displacement, d, is modified. We can define an effective area of diffusion $\sigma(E)$ and

$$\sigma(E) = \frac{\sigma_0}{\bar{l}(E)}, \tag{51}$$

for a finite value of E. We can assume the saturation (with increasing E) value of $\sigma(E)$ which is σ_0 is proportional to $N_h^{-2/3}$.

Hence, one has for the transit time

$$W'_0\, t_T = (N_t \sigma \rho)^{1/\alpha} (L/\bar{l}(E)\rho)^{1/\alpha} \exp(\Delta/kT), \tag{52}$$

where $\rho\sigma \sim N_h^{-1}$, $\rho = (4\pi N_h/3)^{-1/3}$, and $l(E)$ is the mean spatial displacement at each hop. The main change from the ' pure ' hopping case is the reduction of the transition rate pre-factor by the factor $\sim (N_t/N_h)^{1/\alpha}$ and the reinterpretation of Δ, the activation energy

$$\Delta = \Delta_h + \Delta_t, \tag{53}$$

where Δ_h is a hopping energy and Δ_t is the mean trap energy. *Thus, one can relate the observed activation energy to a trap depth, while maintaining a temperature independent dispersion.* This does not preclude a small but significant fluctuation in the trap energy that adds to the dispersion.

Trap-controlled hopping has been observed in molecularly doped organic polymers (Pfister *et al.* 1976). In these systems, a polymer host is doped with

molecules known to activate transport. The trap-controlled hopping process can be verified by proper choice of dopant molecules—for hole transport the difference of ionization potential can be identified with the trap depth—and by proper variation of the concentration of the hopping and trapping sites, (h) and (t), respectively.

2.5. *Monte Carlo simulation*

Numerical simulation represents another approach to the study of the various transport mechanisms. In addition to the analytic studies of multiple-trapping (Pfister and Scher 1977, Schmidlin 1977 b, Noolandi 1977 b), Silver and Cohen (1977) have independently shown the equivalence of multiple-trapping and CTRW using Monte Carlo techniques. They used a distribution of trap-emptying times $\psi(t) \propto (t_0+t)^{-(1+\alpha)}$ and obtained results identical to SM. Marshall (1977) has used numerically generated $I(t)$ results with various trap distributions to fit experimental a-Se data of Pfister (1976 a). The fit was less successful with a-As_2Se_3 data.

Earlier, Silver *et al.* (1971) had used numerical simulation of transient currents to study the effect of various types of bulk trap distributions and surface traps on the shape of $I(t)$. An interesting aspect of these studies was the discussion of delayed surface release, i.e. the time scale of release from surface traps is large compared to the transit time. Therefore, in this case, the shape of $I(t)$ is controlled by the spectrum of surface release times. While this was not pertinent to the dispersive transient currents we are currently investigating, it does have some bearing on the effects of contacts on various transient current responses which will be considered in a later section.

More recently, Silver (1977) has been simulating hopping on a random distribution of sites in an attempt to understand the extent of dispersion in this transport mode. He considers a randomly generated set of sites on a plane with the site at the origin occupied at $t=0$. In each configuration of sites he determines the probability, as a function of time, that the particle will remain within a certain radius R. The configuration average of this probability $Q(t)$ is then obtained for a number of different radii $R=1$, 2, 2·5 (the unit of length is set equal to the mean intersite separation). For $R=1$ he finds $Q(t)$ has a very slow fall-off with t, $Q(t) \propto t^{-\alpha}$ with $\alpha \simeq 0{\cdot}2$. He demonstrates that for $R=2{\cdot}5$ the relative shift, from the $R=1$ curve, along the time axis, is substantial $\sim 10^4$–10^5. He correctly points out that such a large shift is incompatible with random walk or ordinary diffusion theory. The traditional predictions are based on the result that the width of the diffusing packet increases as $t^{1/2}$. However, a CTRW calculation with a $\psi(t) \propto t^{-(1+\alpha)}$ predicts the width of the packet only grows as $t^{-\alpha/2}$ (Shlesinger 1974) in the absence of an applied bias. A calculation based on Shlesinger's (1974) result predicts a shift of $\sim 10^4$ for $R_2/R_1=2{\cdot}5$ and $\alpha=0{\cdot}2$. This is dramatically confirmed by the numerical simulation work of Silver (1977).

The simulation work is still incomplete on the larger question of how much dispersion can be expected for hopping where the randomness is solely due to positional disorder.

2.6. *Percolation approaches*

Percolation theory has been applied to d.c. hopping transport in amorphous solids (Ambegoakar, Halprein and Langer 1971, Pollak 1972). Most notably

these treatments have yielded the Mott $T^{-1/4}$ law. One can obtain the $T^{-1/4}$ law in other models of the hopping transport, e.g. that of Aspley and Hughes (1975).

Pollak (1977) has recently addressed the percolation technique to the time-dependent hopping problem on a random medium. He groups sites into clusters in which all the intersite transition rates $W_{ij}(r)$ are less than some limiting value $W_{ij}(r_m)$ and then assumes that these clusters may be connected with a single spatial link of separation r_m. This reduces the time-dependent problem to motion along a one-dimensional chain with a series of limiting steps each with the same transition rate.

It is not surprising, with such a construction, that one would obtain essentially dispersionless transport. In our opinion, while Pollack (1977) may have implicitly pointed to some limitations in the extent of dispersion due solely to positional disorder, his treatment of the problem, at this point, does not substantially demonstrate this limitation. His basic conclusion is that, for a carrier, if a site is hard to leave, it is hard to enter. Therefore, the hopping carrier avoids all sites which are difficult to enter. This apparent difficulty can be overcome if the hopping is among fluctuating energy levels. Our view is that the anomalous dispersion can be caused by the relatively few long hopping times on the time scale set by the fastest carriers. In other words, most of the carriers must experience a wide dispersion of a statistically small sampling of long hops in order to have non-Gaussian spreading. Of course, the physically isolated site will be avoided but that type of site is not necessary to cause the accumulative spreading in time that we have been discussing.

In fig. 3 of Noolandi (1976) one observes, in the temperature range for non-Gaussian transport, e.g. $T = 143$ K, that the largest transition rate differs from the smallest by a factor of 100. However, the ratio of encounter between the fastest site and the slowest is comparable (~ 25). Hence, one can observe in Noolandi's (1976) fit to the a-Se data the need for a judicious small admixture of the slow sites. The $\psi(t)$, constructed from these parameters, shown in fig. 1 of Noolandi (1977 b), has an algebraic time dependence $\sim t^{-(1+\alpha)}$ only over a two-decade span of time which includes the transit time. This feature re-emphasizes the fact that anomalous dispersion generated by the behaviour of $\psi(t)$ need not have an indefinitely long algebraic tail !

It has been shown that the conductivity corresponding to the percolation path at threshold is zero (Kirkpatrick 1973). One must go beyond threshold where the topology of the path changes rapidly to obtain finite conductivity. There are more interconnections and small cycle loops. The spread in hopping times along such a path is not known at present.

Even with the rather simple path constructed by Pollack (1977), since $W_{ij}(r_m)$ is the rate-limiting step and one assumes that $r_m/R_0 \sim 15$ (cf. § 3.4), one observes that a 30% variation in r_m can give rise to a spread of hopping times of two orders of magnitude. This would be sufficient to disperse the transit time.

In our opinion the controversy of hopping time dispersion on a spatially random distribution of sites reduces to one of degree. The question to be answered is a quantitative one : how much dispersion for a given value of NR_0^3 ?

§ 3. Experimental results and discussion

3.1. *Sample preparation and experimental technique*

All chalcogenide films described in this study were open boat evaporated at a rate of ~ 1 μm/min onto aluminium substrates held approximately at the temperature of the glass transition of the chalcogenide (~ 320 K for a-Se and ~ 450 K for a-As_2Se_3). The films were slowly cooled before transparent top

Fig. 2

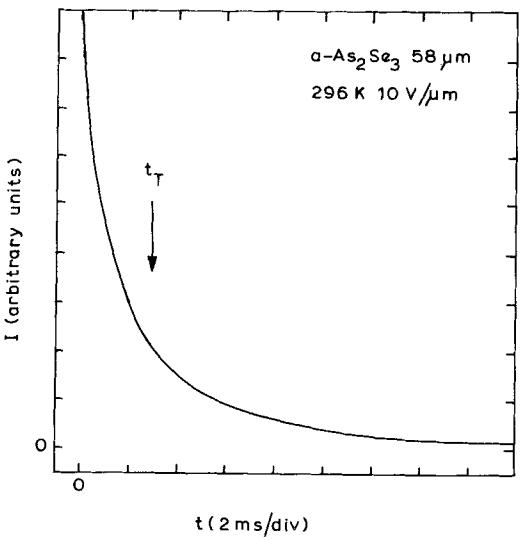

(*a*)

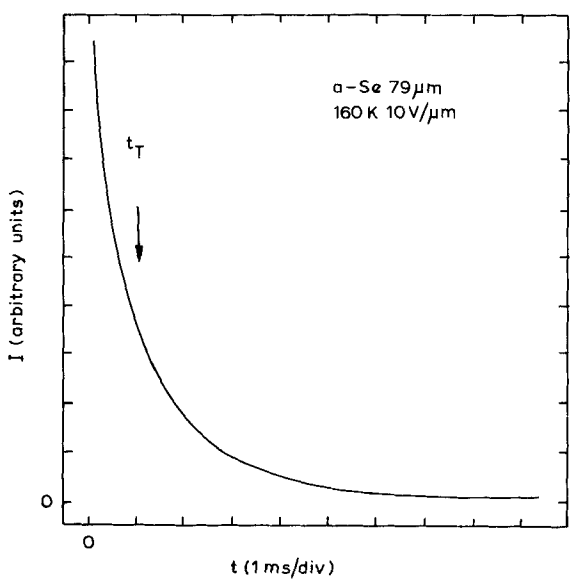

(*b*)

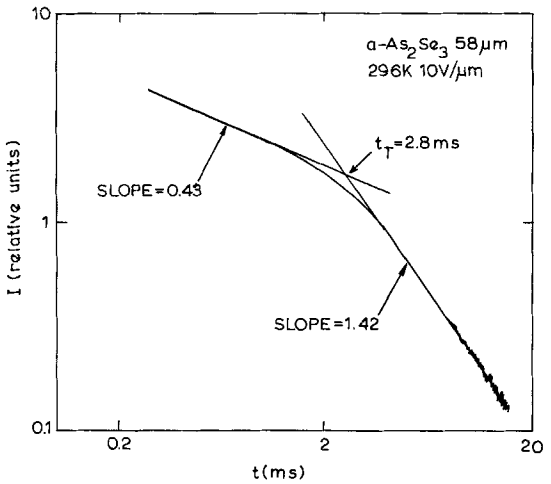

(*c*)

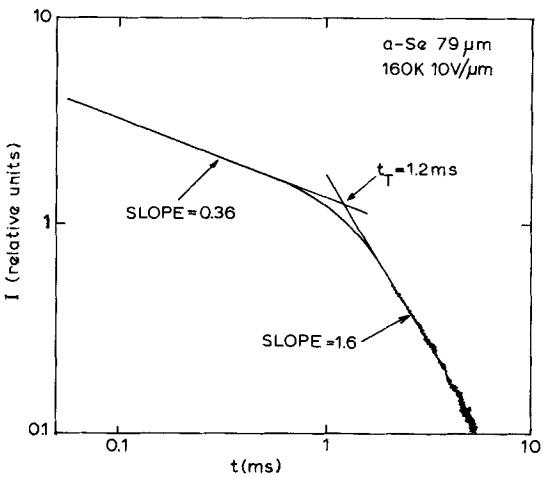

(*d*)

(*a*) Transient hole current in a-As_2Se_3. $L=58\ \mu m$, $T=296$ K, $E=10$ V/μm. Pulse illumination through semi-transparent aluminium (blocking) contact. (*b*) Transient hole current in a-Se. $L=79\ \mu m$, $T=160$ K, $E=10$ V/μm. Pulse illumination through semi-transparent gold contact. Before the application of gold a $\sim 1\ \mu m$ polycarbonate insulating layer was coated onto the selenium sample to provide blocking contact. (*c*) Transient hole current in a-As_2Se_3 of fig. 2 (*a*) in units log I versus log t. (*d*) Transient hole current in a-Se of fig. 2 (*b*) in units log I versus log t.

electrodes were evaporated to obtain a sandwich cell sample structure. The films typically were 5–100 μm thick.

Free carriers were generated by a 5 ns light flash derived from a nitrogen laser which impinged upon the top surface of the sample. Neutral density filters were inserted into the light beam to assure that the injected carrier

density did not exceed $\sim 1/10$ of CV where C is the sample capacitance ($\epsilon = 6{\cdot}4$ for a-Se and 11·2 for a-As_2Se_3) and V the applied voltage. In a typical experiment the light flash lagged the application of the voltage step by about 1/10 of the dielectric relaxation time ($\epsilon_0 \epsilon \rho$). The current transients were stored in a transient digitizer from which plots of $\log I$ versus $\log t$ were generated on an x–y recorder. The transit times were defined by the intersect of tangents approximating $\log I$ versus $\log t$ for $t < t_T$ and $t > t_T$, respectively (eqn. (1)).

3.2. *Experimental manifestation of non-Gaussian and Gaussian transport*

3.2.1. *Current shape*

At room temperatures hole transient currents in a-Se reflect a well-defined charge transit with little dispersion. As the temperature is lowered, the shape of the transient current becomes increasingly featureless, until below ~ 180 K dispersive non-Gaussian transport is observed, which exhibits features similar to room temperature hole transport in the binary glass a-As_2Se_3 (Pfister 1974, 1976). Examples of non-Gaussian transient hole currents for a-As_2Se_3 at room temperature and a-Se at 160 K are displayed for the same field conditions in fig. 2 (*a*) and fig. 2 (*b*), respectively. Clearly both traces deviate strongly from the rectangular pulse shape expected for non-dispersive Gaussian transport. Fig. 2 (*c*) and fig. 2 (*d*) show the same current traces displayed in units $\log I$ versus $\log t$. While in the conventional units I versus t a fiduciary time characteristic of the hole transit is difficult to identify, such a time is readily obtained from the $\log I$ versus $\log t$ traces. In accordance with the predictions of eqn. (1), the transient current can be described by two distinct power law time dependences where the power exponents can be obtained from the slopes of the tangents approximating $\log I$ versus $\log t$ at early ($t < t_T$) and late ($t > t_T$) times of the carrier propagation. Furthermore, the sum of the power exponents is approximately -2, which indicates that for the chosen experimental conditions the probability distribution function for both materials exhibits a power law dependence $\psi(t) \sim t^{-(1+\alpha)}$. From the current traces one derives the disorder parameters $\alpha \sim 0{\cdot}62$ and $\alpha \sim 0{\cdot}5$ for a-Se and a-As_2Se_3, respectively.

Increasing the applied field results in a parallel shift of $\log I$ versus $\log t$ to shorter times and larger currents, which establishes that t_T is a meaningful measure of a carrier transit. Over a wide experimental field range, the logarithmic current plots shift parallel, which confirms that the parameter α indeed is insensitive to the time frame of the experiment (universality of $I(t)$). This feature is best illustrated in a plot where transient currents recorded for a wide range of transit times are superimposed by shifting along the logarithmic axes to produce a master plot. Examples of master plots are shown in fig. 3 (*a*) for a-As_2Se_3 at room temperature and fig. 3 (*b*) for holes in a-Se at 143 K. The dashed lines in fig. 3 (*a*) indicate the relative spread σ/l expected for Gaussian transport for the longest and shortest transit time. The α values obtained from the master plots are $\alpha \sim 0{\cdot}45$ for a-As_2Se_3 and $\alpha \sim 0{\cdot}53$ for a-Se. Master plots similar to those shown in fig. 3 have been observed for hole transport in doped organic polymers (Mort *et al.* 1976, Pfister *et al.* 1976, Pfister 1977), carbazole polymers (Pfister and Griffiths 1978), the charge transfer complex of poly(*N*-vinylcarbazole) : trinitrofluorenone (Seki 1974) and amorphous SiO_2 (Hughes 1977, McLean *et al.* 1975).

Fig. 3

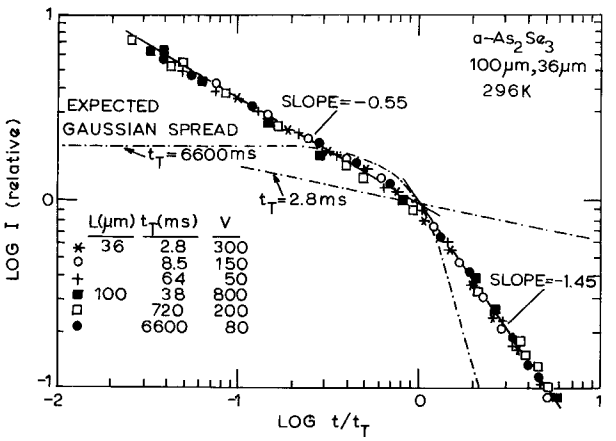

(*a*)

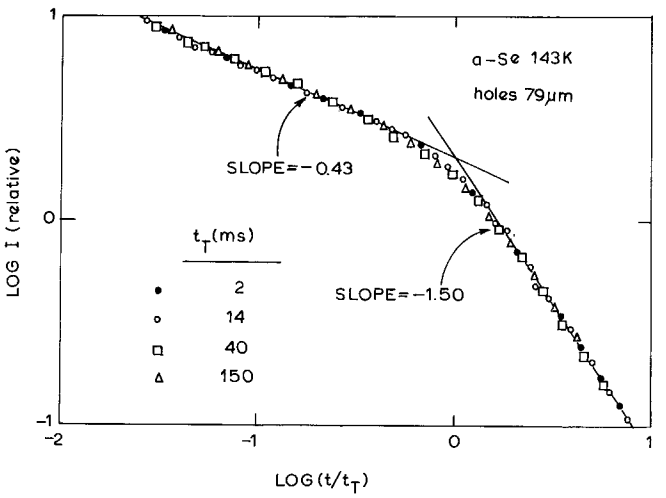

(*b*)

(*a*) Master plot for transient hole currents in a-As_2Se_3. $L=100$ μm, 30 μm, $T=296$ K. Plot was obtained by shifting along the logarithmic axes of individual traces recorded at different bias fields. Transit times are listed in the legend. The broken lines indicate the relative spread expected for Gaussian transport in which case $\sigma/l \sim t_T^{-1/2}$ (after Pfister and Scher 1977 a). (*b*) Master plot for transient hole currents in a-Se. $L=79$ μm, $T=143$ K. Plot was obtained by shifting along the logarithmic axes of individual traces recorded at different bias fields. Transit times are listed in the legend (after Pfister 1976 a).

The algebraic time dependence of the transient current $I(t)$ given in eqn. (1) approximates the experimental current traces in the time range $\sim 0{\cdot}1t_T$ to $10t_T$. At much shorter times the current typically falls off faster than predicted for $\psi(t) \propto t^{-(1+\alpha)}$. There are many possible explanations for this behaviour. For one thing, at these early times of the transit the carriers drifted over a

Fig. 4

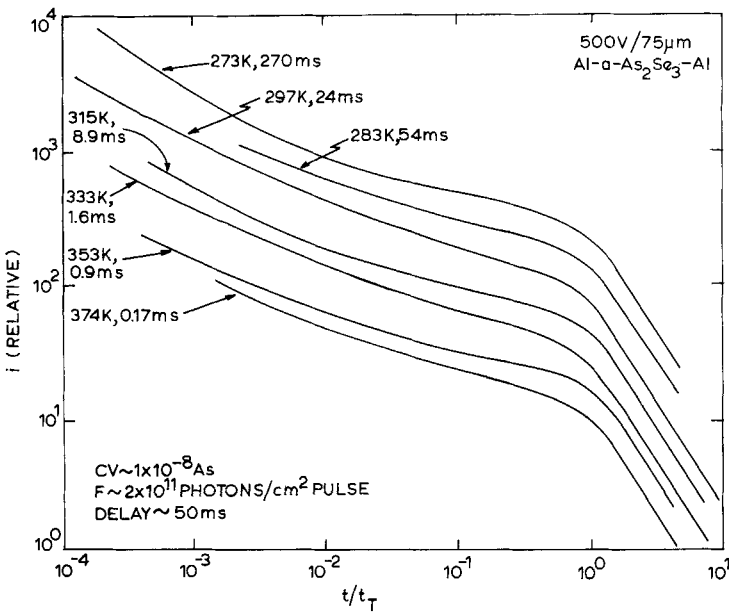

(*a*)

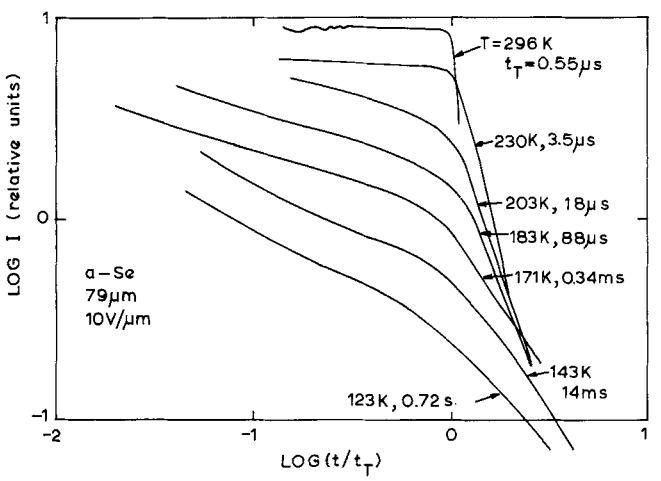

(*b*)

(*a*) Temperature dependence of transient hole current shape in a-As_2Se_3 at 6·7 V/μm.
(*b*) Temperature dependence of transient hole current shape in a-Se at 10 V/μm.

distance much less than the sample thickness and the development of the dispersion may be dominated by surface effects which are believed to play a role in chalcogenides. Another possibility is that the time dependence of the distribution function cannot be described by a simple power law with constant

exponent over many orders of magnitude of t_T. As will be discussed later, hole transients in a-Se indeed reflect the limited time range over which $\psi(t) \propto t^{-(1+\alpha)}$.

The shape of the transient current for a-As_2Se_3 is remarkably stable with respect to temperature. This is demonstrated in fig. 4 (*a*), where current traces recorded over a wide range of temperatures are shown in normalized time units. In contrast with this behaviour, the hole traces for a-Se shown in fig. 4 (*b*) show a progressive increase of the dispersion as the temperature is lowered. Both these observations will have implications on the underlying microscopic transport mechanisms (§ 4).

3.2.2. *Thickness dependence*

For transient transport with Gaussian dispersion, the drift mobility is well defined, hence the transit time increases in proportion to the sample length.

Fig. 5

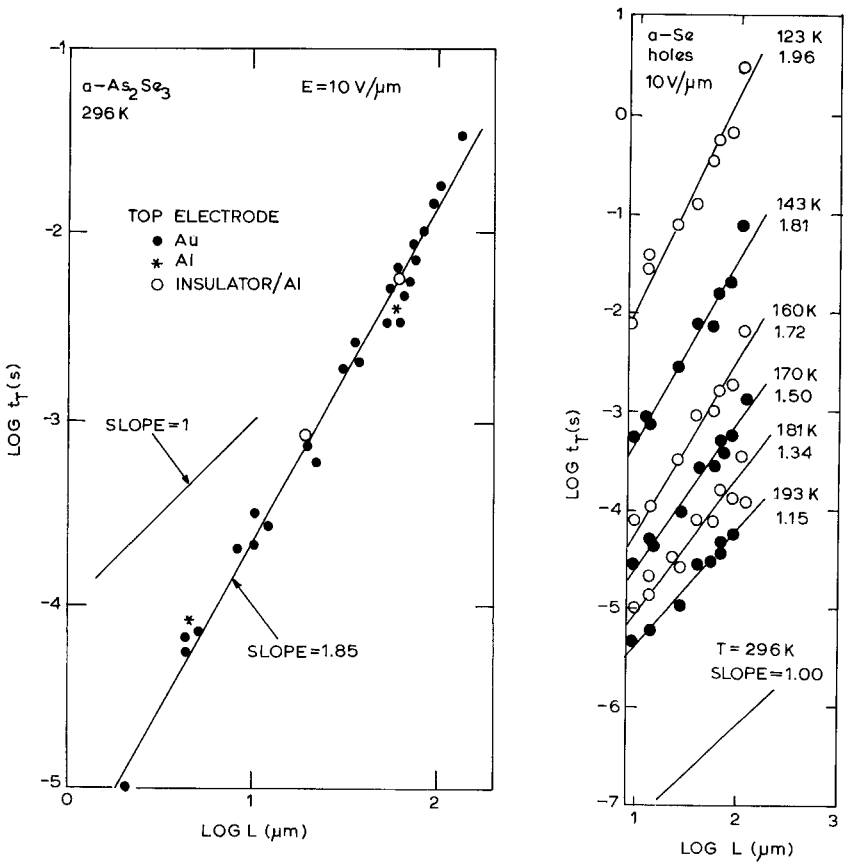

(*a*) (*b*)

(*a*) Thickness dependence of transit time t_T for hole transport in a-As_2Se_3 at 10 V/μm and 290 K (after Pfister and Scher 1977 a). (*b*) Thickness dependence of transit time t_T for hole transport in a-Se at 10 V/μm at various temperatures (after Pfister 1976 a).

This is not the case for non-Gaussian transport, where the drift velocity decreases with time. The resulting superlinear thickness dependence of the transit time is clearly manifested in fig. 5 (*a*) for hole transport in a-As_2Se_3 at room temperature. Using the theoretical prediction, eqn. (2), one obtains from fig. 5 (*a*) $\alpha \sim 0{\cdot}55$ which is in remarkable agreement with the value obtained from the shape of the transient current. For holes in a-Se the superlinear thickness dependence is observed at lower temperatures where transport becomes non-Gaussian (fig. 5 (*b*)). At higher temperatures ($T > 180$ K), the transit time scales with thickness as is expected for a well-defined drift mobility.

The ramnifications of the thickness dependence clearly are that in the region of dispersive transient transport, a conventional definition of the mobility is not possible. Hence, any correlation of steady-state dark conductivity, σ_{dc}, and transient measurement is not obvious. Indeed, it will be shown in the next paragraph that at low fields σ_{dc} and t_T display distinctly different field dependences which further demonstrates the implications of non-Gaussian transport.

3.2.3. *Field dependence*

Whereas the thickness dependence of t_T is rigorously determined by the statistics of the transport process, the field dependence cannot be obtained without further assumption. This amounts to a more detailed description of the field dependence of the mean displacement $l(E)$ between events. To a first approximation one can reasonably assume $l \propto E$ in which case eqn. (2) reduces to

$$t_T \sim \left(\frac{L}{E}\right)^{1/\alpha} \exp(\Delta/kT). \tag{54}$$

Higher order terms in the expansion of $l(E)$ can be introduced to obtain stronger field dependences. For instance, assuming an exponential field dependence of the transition probabilities between successive events in the case of hopping transport leads to (Pfister 1977 a, b)

$$t_T \sim L^{1/\alpha}\left[\sinh\left(\frac{e\rho E}{2kT}\right)\right]^{-1/\alpha} \exp(\Delta_0/kT), \tag{55}$$

where ρ is the average distance between hopping site of density N_h ($\rho \simeq (3N_h/4\pi)^{-1/3}$) and Δ_0 is the activation energy at $E = 0$. At low fields, $eE\rho/2kT \ll 1$, eqn. (55) approaches the earlier result, eqn. (54). At high fields, $e\rho E/2kT \gg 1$, hence

$$t_T \sim L^{1/\alpha} \exp(\Delta_0/kT) \exp\left(-\frac{e\rho E}{2\alpha kT}\right), \tag{56}$$

i.e. the activation energy approximates a linear field dependence

$$\Delta = \Delta_0 - e\rho E/2k\alpha$$

which is determined by the hopping site distance and the disorder parameter α. The high field approximation in eqn. (56) is identical to a treatment of transport in one dimension in the presence of fluctuating potential barriers (Funabashi and Rao 1976). At low fields, however, the one-dimensional treatment predicts $t_T \propto E$, implying field independent transport, whereas the formula based on the

three-dimensional treatment of SM predicts the power law field dependence, eqn. (54). Thus disorder prevents transient transport from becoming field-independent even at the lower fields as long as $\psi(t) \propto t^{-(1+\alpha)}$ is a good approximation to the probability distribution function.

Fig. 6

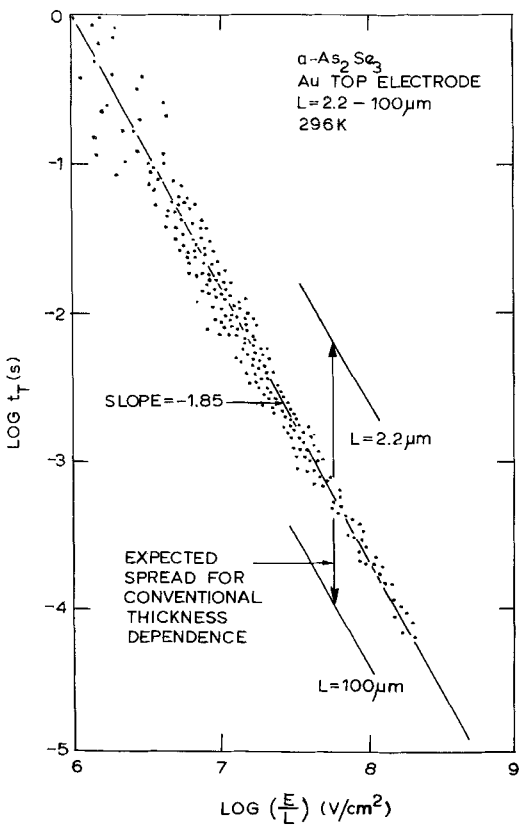

(E/L)-dependence of transit time for hole transport in a-As_2Se_3 at room temperature. Range of sample thicknesses 2·2–100 μm. Field range 2–10 V/μm (after Pfister and Scher 1977 a).

The low-field approximation, eqn. (54), lends itself to a direct comparison with the experiment. That is, a plot of $\log t_T$ versus $\log (E/L)$ should yield a straight line of slope $1/\alpha$ which is independent of sample thickness and applied field (low enough for eqn. (54) to hold). The result is shown in fig. 6 for a-As_2Se_3 at room temperature for samples ranging in thickness from 2·2 μm to 100 μm. The different data produce a master curve which has an average slope of $-1{\cdot}85$ yielding $\alpha \sim 0{\cdot}55$. This value agrees remarkably well with earlier estimates (fig. 5 (*a*), fig. 3 (*a*)). The linear t_T versus E/L expected for the Gaussian transport for the extreme sample thicknesses is indicated to illustrate the clear deviation from the conventional case.

Fig. 7

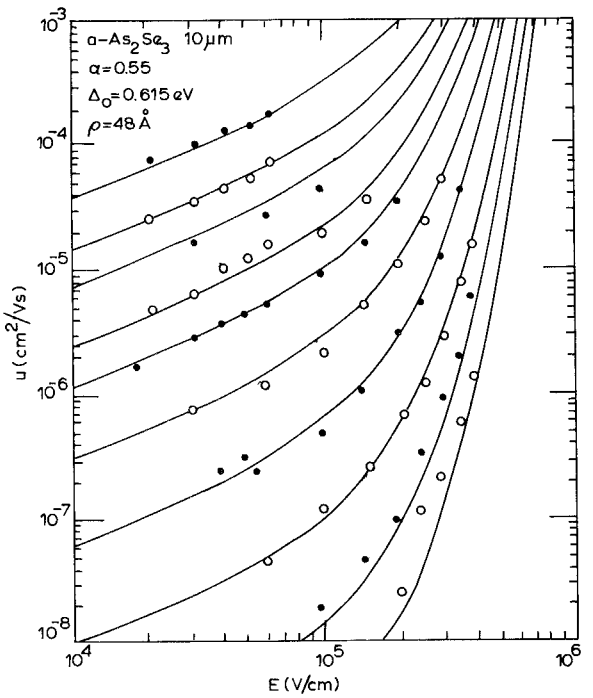

Field dependence of hole mobility in 10 μm thick a-As_2Se_3 sample at various temperatures. The lines were calculated from eqn. (55) using the parameters listed in the figure (after Pfister 1977 b).

At higher fields the field dependence of t_T becomes stronger than $E^{-1/\alpha}$. Fig. 7 shows data for a-As_2Se_3 over a wide field and temperature. The fitted lines represent eqn. (55) calculated for the parameters listed in the figure. Again the disorder parameter agrees well with earlier estimates. The application of eqn. (55) to the hole transport data for a-As_2Se_3 implies a hopping mechanism, a subject which will be dealt with in § 4. The hopping distance for various samples ranged between $\sim$4–5 nm which yields a hopping site density $N_h \sim 10^{18}$–10^{19} cm^{-3}.

3.2.4. *Temperature dependence*

Transient hole transport in a-As_2Se_3 is thermally activated with well-defined activation energy which at low fields has the average value $\sim$0·62 eV (Fisher *et al.* 1976, Pfister and Scher 1977). This large value indicates that the propagating hole packet interacts with a density of localized state located several tenths of an eV below the hopping transport states. The resulting transport mechanism has been termed ' trap-controlled hopping ' (§ 3 ; Pfister *et al.* 1976, Pfister and Scher 1977). Early experiments on thin films of a-As_2Se_3 yielded an activation energy of 0·45 eV which was interpreted to indicate the existence of a second less deep hole trapping level (Marshall and Owen 1971). It was argued that for thin films and correspondingly short transit times

($< 0{\cdot}1$ ms), the holes interact only with the shallower level at $\sim 0{\cdot}45$ eV and that the superlinear thickness dependence of the transit time arises because for thicker samples the carriers interact with progressively deeper-lying traps (Fisher *et al.* 1976).

Fig. 8

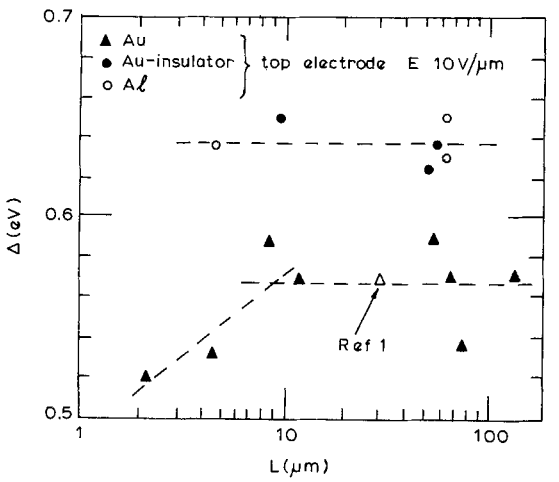

Low field activation energy for hole transport in a-As_2Se_3 for various sample thickness and electrodes (after Pfister and Scher 1977 a).

We do not concur with this explanation for the observed transit time dispersion and associated non-Gaussian behaviour of the pulse shape and transport parameters. While it is true that the activation energy for hole transport in a-As_2Se_3 drops as the evaporated films become thinner (fig. 8), the dispersion of the pulse shape and the superlinear thickness dependence of the transit time persists for $L > 10$ μm, where the activation energy approaches a constant value. It is also seen from fig. 4 (*a*) that the current at early times of the transient exhibits the same temperature dependence as the post-transit time current which would not be expected if the carriers were to interact with progressively deeper-lying traps as they penetrate the bulk of the sample.

It is interesting to note from fig. 8 that the activation energy measured with Au as an illuminated electrode is smaller than with Al. Dark current injection measurements have established that Au is capable of injecting more charge into a-As_2Se_3 than Al (Abkowitz and Scher 1977) and the dark d.c. level measured with Au exceeds that measured with Al by about one order of magnitude. Since Au is more injecting than Al, it is possible that the dark Fermi level in the former lies closer to the transport states. If the Fermi level lies close to the 0·62 eV trapping level and the screening length is of the order of the sample thickness, the observed variation of the activation energy with the metal contact and sample thickness could indeed be rationalized. More detailed studies of this effect with different contact material would be desirable.

An interesting explanation for a thickness-dependent activation energy is offered by the non-Gaussian transport theory. As discussed in § 2.2, the dispersion parameter α becomes temperature-dependent if the carriers interact with traps that are distributed in energy. Combining eqns. (54) and (50) leads to

$$\Delta \simeq \Delta_0 + kT_0 \ln (L/L_0) ; \tag{57}$$

hence a temperature-dependent dispersion generates a thickness dependent activation energy. For a-As_2Se_3 $d\alpha = dT/T_0 < 0{\cdot}15$ for $dT \sim 100$ K, hence $T_0 \gtrsim 670$ K. With these values, one estimates that the activation energy for a 100 μm thick sample is $\sim 0{\cdot}2$ eV larger than that for a 2 μm thick sample.

Fig. 9

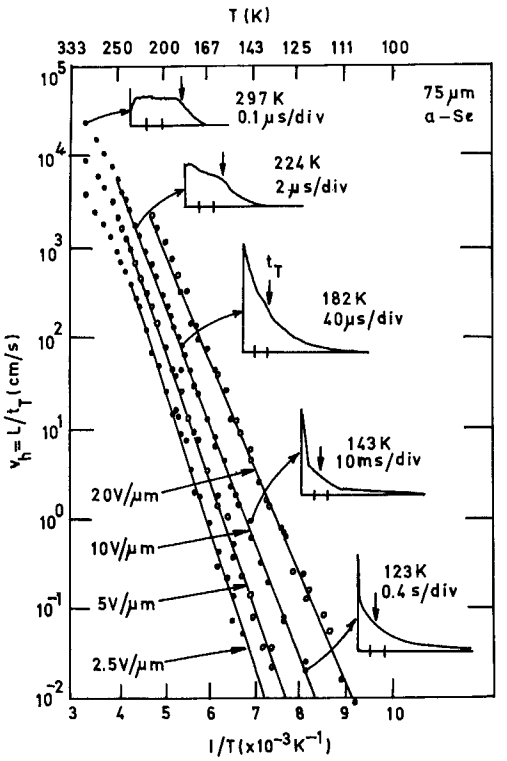

Temperature dependence of hole velocity in a-Se at different fields. Several representative current traces are shown for 10 V/μm (after Pfister 1976 a).

With respect to a-As_2Se_3, hole transport in a-Se exhibits some novel features. As shown in fig. 4 (*b*), the current shape, which at room temperature is typical of a well-defined charge drift becomes progressively dispersive as the temperature is lowered and below ~ 180 K exhibits the signature characteristic of non-Gaussian transport. Fig. 9 shows that this transition from non-dispersive to dispersive transport is not accompanied by a change of the

activation energy which indicates that the same basic transport mechanism prevails over the entire temperature range (Pfister 1976). The deviation from the Arrhenius temperature dependence at ~ 250 K is believed to be associated with the glass transition temperature. In fact, extending the temperature range to ~ 320 K demonstrates that the hole mobility becomes temperature-independent above ~ 300 K and does not reflect a T^{-n} behaviour (Abkowitz and Pai 1978).

3.2.5. *Correlations between* $t_T(E, L)$ and $I(t)$

The dispersion of the transient current and the disorder-induced thickness and field dependence of the transit time are correlated via the parameter α of eqns. (1) and (2). That correlation constitutes an important test of the non-Gaussian transport model and can readily be studied for hole transport in a-Se.

Figure 10 shows the dispersion parameter α as a function of temperature. α_L was determined from the thickness dependence of t_T (fig. 5 (*b*)). α_i and α_f were determined from the slopes of the pulse shape at times $t < t_T$ and $t > t_T$, respectively (fig. 4 (*b*)). In terms of these parameters, the Gaussian régime can be characterized by $\alpha_L = \alpha_i = 1$ and $\alpha_f \gg 1$ while non-Gaussian transport governed by $\psi(t) \propto t^{-(1+\alpha)}$ can be described by $0 < \alpha_L = \alpha_i = \alpha_f < 1$. Figure 10 clearly demonstrates the approach from Gaussian to non-Gaussian behaviour in terms of these parameters in the temperature range 140–160 K. Below 140 K $\alpha_L \simeq \alpha_i \sim 0{\cdot}55$ whereas α_f rapidly falls off to approach a value of $\sim 0{\cdot}15$. The temperature dependence of α and the different behaviour of α_i, α_f and α_L suggests that $\psi(t)$'s were more complicated than originally suggested by SM

Fig. 10

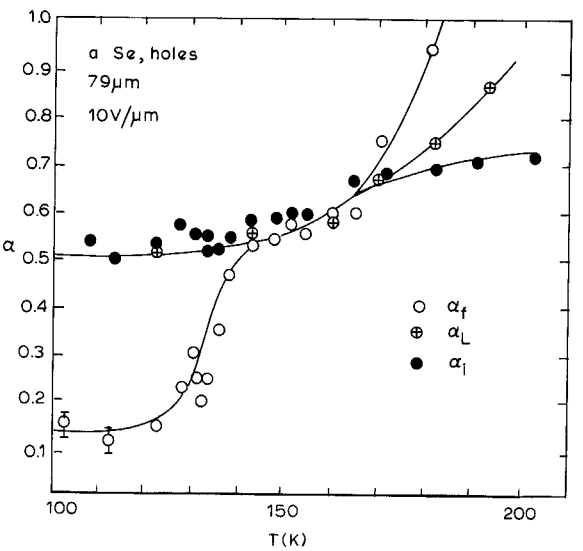

Temperature dependence of parameter α for hole transport in a-Se determined from thickness dependence of transit time, α_L, initial and final part of current trace, α_i and α_f, respectively (after Pfister 1976 b).

must be used to explain these transport data. Such $\psi(t)$'s have recently been obtained from a fit of a parametrized multiple-trap analysis (Noolandi 1977, see § 4).

Unlike a-Se, for a-As_2Se_3 a temperature variation cannot be utilized to establish the predicted correlations. However, these correlations could be established by comparing the power exponent obtained from the field dependence of $t_T(=1/\alpha_E)$ and the average α-value, determined from the current shape, $\alpha_I = 1/2(\alpha_i + \alpha_j)$. Again, for the non-Gaussian case where $\psi(t) \propto t^{-(1+\alpha)}$ one expects $\alpha_E = \alpha_I = \alpha_L$. Figures 2 (*c*), 3 (*a*), 4 (*a*), 5 (*a*) and 6 indeed establish this correlation. A more detailed test could be performed following the observation that the field dependence of the transit time varied among various samples although they were prepared under identical evaporation conditions. As is shown in fig. 11, the variation of α_E is correlated with a variation of α_I.

Fig. 11

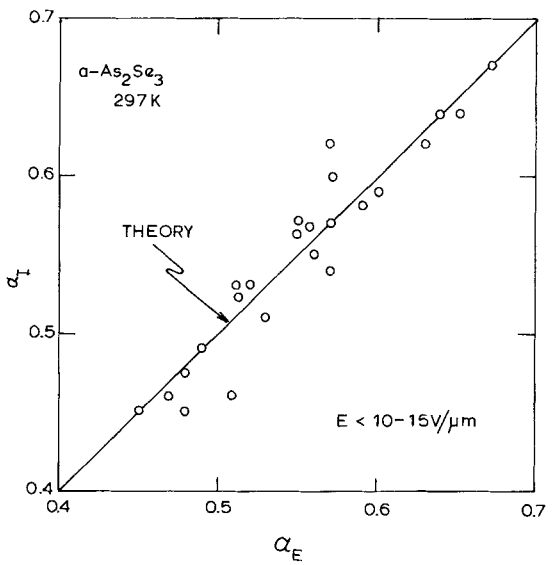

Correlation between current shape and field dependence for hole transport in a-As_2Se_3 at room temperature. $\langle\alpha_I\rangle$ is average α-value determined from current shape, α_E is determined from field dependence of transit time (after Pfister 1976 b).

3.3. *Dark d.c. conductivity and contacts*

The field and temperature dependence of the dark d.c. conductivity in many disordered systems can be explained by the empirical form (Marshall and Miller 1973, Fisher *et al.* 1976)

$$\sigma_{dc}(T) = \sigma_0 \exp(-\Delta_0/kT) \exp(ea(T)E/kT). \tag{58}$$

Indeed dark conductivity measurements on a-As_2Se_3 with gold contacts confirm this expression over a wide field and temperature range. Since σ_{dc} is obtained from a steady-state measurement, the mobility $\mu = \sigma/ne$ is well defined and

Fig. 12

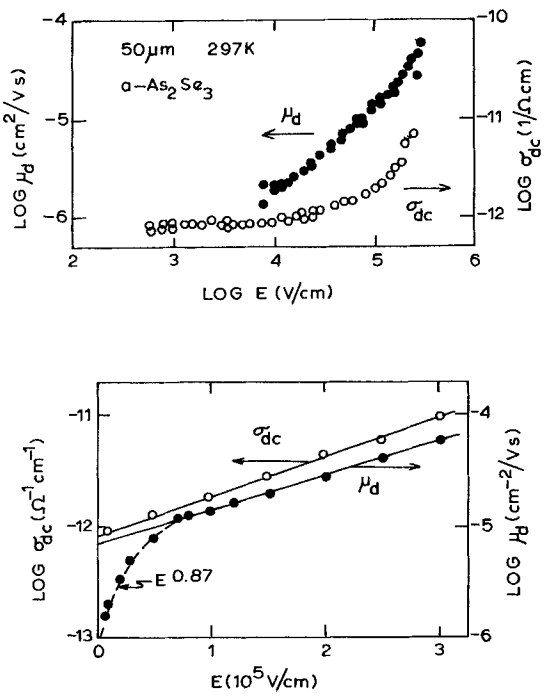

D.c. conductivity and hole mobility versus field in a-As_2Se_3. $L=50\ \mu m$, $T=297$ K (after Pfister and Scher 1977 a).

should not exhibit the field and thickness dependence of the mobility derived from the non-Gaussian transient current. In agreement with this prediction, σ_{dc} is found to be an intrinsic variable (independent of sample thickness). Furthermore, as shown in fig. 12, the field dependence of σ_{dc} at low fields is much weaker than the field dependence of the transient conductivity. The different behaviour of the steady-state and transient conductivities then constitutes a beautiful example to demonstrate the relation between the distribution of statistical event times and the observation time. Interestingly, at high fields both σ_{dc} and μ_d, operationally defined as $L/t_T E$, approach the same exponential field dependence exp (eaE/kT), where the coefficient a is approximately the same for both measurements (fig. 12). While this could mean that disordered induced fluctuations are overcome in the presence of strong fields, the field independence of α does not support this view.

An interesting consequence follows from the fact that the steady-state and transient conductivities exhibit the same field dependence above some limiting field (~ 10 V/μm for a-As_2Se_3 at room temperature). An exponential field dependence at high fields is indeed predicted for the transient conductivity (eqn. (55)). An exponential high field dependence is also predicted for the steady-state conductivity from a one-dimensional analysis of carriers hopping over fluctuating barriers (Funabashi and Rao 1976). In fact, the predicted exponential field dependences are formally equivalent if one equates $\alpha=1/s$

where α is the disorder parameter in the SM transport theory and s is a measure of the fluctuation of the potential barriers between localized sites. Now, α describes the time evolution of the propagating carrier packet and itself is time dependent (eqn. (50)).

The parameter s, on the other hand, describes a steady-state situation and therefore is time independent. It remains a challenge for future theoretical work to explain why at high fields both transient and steady-state conductivities approach the same field dependence with $\alpha \simeq 1/s$. The formula of Funabashi and Rao (1976) predicts that the field dependence of the d.c. conductivity sets in when $e\rho Es/2kT > 1$. Note that the deviation from the power law field dependence of the transit time, $E^{1/\alpha}$, is expected to occur at a higher field since the parameter α does not enter the argument of the sinh function of eqn. (55). This is supported by the experimental data shown in fig. 12.

Some additional remarks are appropriate in the discussion of d.c. dark currents in highly insulating solids. The important role the contact may play in these measurements is well appreciated when dealing with crystalline semiconductors but they have received little attention in characterizing the electrical properties of disordered solids. Ideally, the contact used for d.c. measurements should be invisible (i.e. ' ohmic ') such that the d.c. current flowing through the sample for a fixed external field is determined only by the transport parameters of the solid. Most often ohmic contacts are difficult to realize and by using the technique of four-probe measurements the non-ohmicity of the contacts can be circumvented. However, for highly insulating solids or solids with appreciable surface conductivity, this technique can lead to erroneous results and one has to rely on bulk conductivity measurements performed on thin sample films which are provided with electrodes on both sides (sandwich cell configuration). To be able to interpret this type of data which typically consists of a family of plots of d.c. current versus applied field, j versus E, one first has to establish the nature of the contact. This may be complicated by the additional problem that the contact may change its properties as a function of time following the application of the external field. In the following some procedures are outlined that should enable one to distinguish among ohmic and non-ohmic (emission-limited) contacts.

An ohmic contact must satisfy two stringent conditions. The first is contact invisibility when the applied field is sufficiently low such that any excess injected carrier is neutralized before it completes the transit across the film. Under these conditions, the resident carrier density, n, is presumed to be unperturbed by the contact and only under these conditions can a d.c. current be interpreted as $j = \sigma E$, where $\sigma = en\mu$. μ is the microscopic mobility. The second condition is that when the field is high enough such that any excess injected carrier completes the transit before it is neutralized, the ohmic contact behaves like a perfect injector with an unlimited carrier reservoir to supply a space-charge-limited current (SCLC). The transition between the high and low field behaviour is expected to occur at fields for which the transit time $t_T = L/\mu E$ approaches the dielectric relaxation time (Maxwell time) $\tau = \epsilon_0 \epsilon \rho$, where ρ is the unperturbed bulk resistivity and ϵ the dielectric permittivity. Taking a-As_2Se_3 as an example, the transition into space-charge-limited conditions is expected for fields $E \gtrsim L/\rho\epsilon_0\epsilon\mu \sim 0{\cdot}1$ V/μm for a 100 μm thick sample film assuming $\rho \sim 10^{13}$ Ω cm, $\epsilon = 11{\cdot}2$ and $\mu \sim 10^{-5}$ cm^2/V s.

Fig. 13

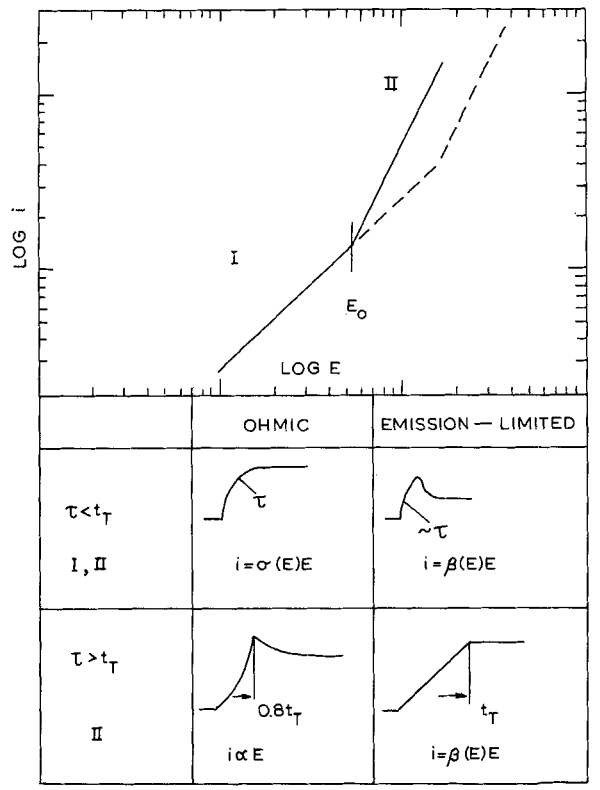

Schematic j–E characteristic and current responses to a voltage step for ohmic and emission-limited contacts (see text).

Consider the schematical j–E plot in fig. 13, which consists of a linear part $j \propto E$ at low fields $E < E_0$ and a superlinear part $j \propto E^n$ at fields $E > E_0$. j–E plots of the type shown are typically found in dark conductivity measurements in disordered solids, of which a-As_2Se_3 represents a well-known example. If the increased field dependence for $E > E_0$ is due to space-charge limitation, the critical field E_0 increases in proportion to the sample thickness L. (The transition to SCL occurs when $t_T \sim \tau = \rho\epsilon\epsilon_0$, i.e. $E_0 \sim L/\mu\tau$.) Hence, changing the sample thickness provides a straightforward method to check the ohmicity of the contact and the origin of the superlinear field dependence (dashed line in fig. 13). If, however, the j–E plots for different sample thicknesses scale in units of j versus E, one has to resort to alternative techniques to determine the properties of the contact. If the contact is *ohmic* and the current for $E > E_0$ is not space-charge-limited, the j–E curve reflects a field-dependence d.c. conductivity, $\sigma(E)$. If the contact is *emission-limited*, the d.c. current level is determined by the rate the contact can supply carriers and, therefore, the j–E curve represents the field dependence of the carrier supply. Ohmic contacts can be distinguished from emission-limited contacts

by examining the time evolution following the application of a step-voltage (Scher *et al.* 1971).

If the contact is ohmic, the time to establish current equilibrium following the application of an external field is determined by the dielectric relaxation time, $\tau = \epsilon_0 \epsilon \rho$, or the RC time of the electronic circuit if $RC > \tau$ (compare the schematic current responses in fig. 13). If for $E > E_0$ the d.c. current shows the thickness dependence characteristic for space-charge limited currents, then the current response following a field step $E > E_0$ should exhibit the cusp well known from transient space-charge-limited currents. However, unlike the photo-induced transient current which approaches zero (i.e. dark level) for $t > t_T$, the current induced by the step field should asymptote to the space-charge-limited dark current. If neither of the current responses illustrated in fig. 13 for ohmic conditions is observed, the contact has to be emission-limited. For $\tau > t_T$ it takes a transit time to establish the (emission-limited) d.c. current and therefore, as shown in fig. 13, the current response is a ramp of width t_T.

Fig. 14

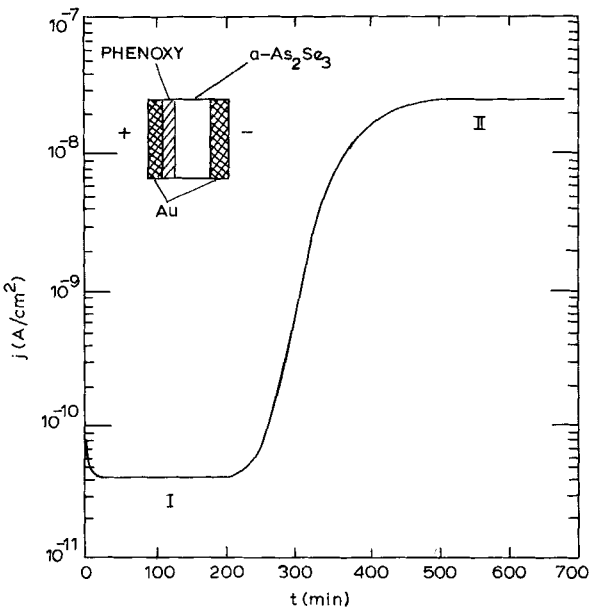

Time-dependent behaviour of gold/phenoxy contact on a-As_2Se_3 following the application of the applied field at $t = 0$. Region I : emission-limited contact ; Region II : contact characteristic of gold (after Tutihasi 1976).

The contact may change its characteristics as a function of time following the application of the step field or as a function of the field strength. Figure 14 depicts as an example the time dependence of the dark current for a-As_2Se_3 for the electrode configuration shown in the insert (Tutihasi 1976). The current exhibits a distinct S-shape time dependence with a rapid rise occurring at $t_0 \sim 250$ min. The characteristic time t_0 decreases with increasing field and

temperature. A similar S-shape time-dependence is observed if the sample is photoexcited with strongly absorbed light. The detailed examination of this time-dependence indicates that the gold/phenoxy contact changes from an emission-limited contact of very low injection efficiency ($\sim$blocking) to a contact characteristic of gold on a-As_2Se_3. The transition between the two régimes occurs when the electric field across the phenoxy layer due to the electrons trapped at the phenoxy/a-As_2Se_3 interface is sufficiently intense to promote hole tunnelling from gold into a-As_2Se_3. It is suggested that similar electrode effects are important for the time-dependence of the photocurrent observed in a-As_2Se_3 and other chalcogenide glasses provided with aluminium or SnO_2 contacts (Kolomiets *et al.* 1973).

The techniques described in fig. 13 to determine the properties of contacts have been successfully applied in a study of the behaviour of gold on a-As_2Se_3 (Abkowitz and Scher 1977, Abkowitz and Scharfe 1977). Gold is most commonly used in j–E measurements and the results have been interpreted in terms of $j=\sigma E$ which implies that the gold contact is ohmic (see for instance, Hurst and Davis 1974). Paradoxically, using the same contact, time-resolved photoinduced hole transients can be observed in a-As_2Se_3, which implies that the contact exhibits non-ohmic behaviour. The hole transients can be excited after the dark current equilibrium has been established, precluding any possibility of the contact relaxing from initially blocking to finally ohmic after the onset of the field. The step-field experiments confirm the perception obtained from time-of-flight experiments that gold forms not an ohmic but an emission limited contact, at least for fields where time-of-flight experiments can be performed ($\gtrsim 1\times 10^4$ V/cm at room temperature). The time evolution of the current following the application of the field is initiated by the transit of a finite charge stored at the gold contacts/a-As_2Se_3 interface. Under steady-state conditions, the charge reservoir at the interface becomes depleted and the current value is determined by the rate carriers are emitted from the gold contact (Abkowitz and Scher 1977). Interestingly this rate appears to reflect bulk transport properties determined from time-of-flight measurements. The correlation of the field and composition dependence of the drift mobility and dark d.c. conductivity in a-As–Se alloys at high fields is well recognized and, initially, led to the presumption that the dark current in these systems is ohmic in the sense that $j=en\mu E$. The step-field experiments indicate that the relationship between d.c. current and bulk transport parameters is more complicated and needs further investigation.

Typical current responses following the application of a voltage step are shown in fig. 15 for a variety of experimental conditions. The time t_m of the current maximum exhibits the field and temperature dependence of the transit time t_T determined from time-of-flight experiments. The various experimental conditions were chosen to demonstrate that the surface charge reservoir is depletable, depends upon the interface and can be restored by surface-absorbed light. The detailed time-dependence of the current response at $t\sim t_m$ can be accounted for by a model that convolutes a time-dependent depletable surface charge reservoir with the stochastic (non-Gaussian) transport properties described in § 2 (Abkowitz and Scher 1977). In addition, this model accounts for the offset in value of the transit time determined by time-of-flight and by the response to a step in voltage.

Fig. 15

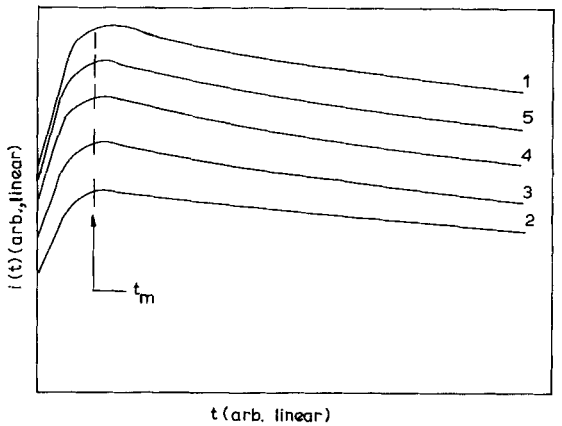

Current response to a 500 V voltage step of a gold/a-As_2Se_3 sandwich cell $L = 100$ μm, at room temperature, for various resting periods following the application of the field. The field was on for 60 s and then off for 5 min after which trace (1) was recorded. Following a 5 min rest the field was on for 60 s and then off for 15 s after which trace (2) was recorded. This sequence was repeated for 30 s, 60 s and 120 s resting periods, trace 3, 4 and 5, respectively. The sequence 3–5 demonstrates the relaxation of the depleted contact (2) towards the relaxed contact (1) (after Abkowitz and Scher 1977).

3.4. *Dispersive transport in disordered solids other than chalcogenide glasses*

3.4.1. *Organic disordered solids*

Non-Gaussian transport is not specific to chalcogenide glasses but has been observed in a broad range of disordered solids, both inorganic and organic. The organic solids offer the enormous experimental advantages that the states involved in transport can easily be controlled by materials preparation. Thus hopping transport which prevails in all organic disordered materials studied so far can readily be identified on the basis of the exponential dependence of the transit time on the average distance between localized sites which can be controlled chemically. Hence a study of the organic disordered solids such as carbazole polymers (Gill 1972, Pfister and Griffiths 1978), molecularly doped polymers (Montroll 1976, Pfister *et al.* 1976, Pfister 1977 a) and organic amorphous glasses (Gill 1974) should provide some detailed information on the mechanisms underlying the charge transfer between localized states. In the following a brief survey of experimental data pertinent to non-Gaussian transport will be presented. Emphasis will be on the fact that the transport properties of these systems and the chalcogenide glasses are very much alike, and thus provide unique models of hopping transport against which modes of transport proposed for the chalcogenide glasses can be compared and analysed.

Dispersive transient hole and electron transport has been observed for the charge transfer complex of poly(*N*-vinylcarbazole) with trinitrofluorenone (Gill 1972) and, like for a-As_2Se_3, a plot of log I versus log t showed the universality behaviour characteristic of non-Gaussian transport (Seki 1973). Similar master plots could be produced from transient hole current in molecularly doped

polymers (Mort *et al.* 1976, Pfister 1977 a). A specific example for a solid solution of *N*-isopropylcarbazole in polycarbonate is shown in fig. 16.

Transport in the disordered organic systems occurs via hopping among localized sites associated with the dopant molecule. Most commonly charge transport is unipolar with hole transport prevailing when the dopant molecule is donor-like, while electron transport is more common for acceptor molecules. On a molecular level, charge transfer can be viewed as a redox process in which a neutral molecule transfers an electron to a neighbouring molecular cation

Fig. 16

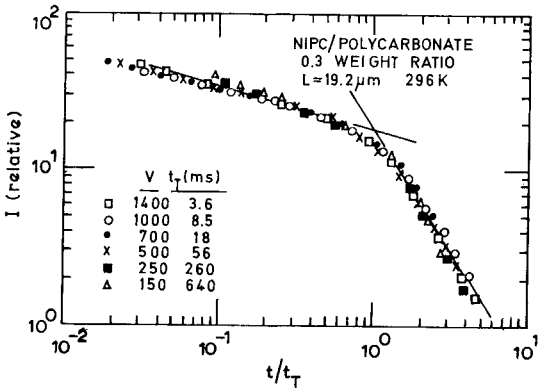

Master plot for hole transient current in molecularly doped polymer *N*-isopropylcarbazole/polycarbonate NIPC/Lexan (after Mort *et al.* 1976).

(hole transport) or from an anion to a neighbouring neutral molecule (electron transport). Hence, the transit time measured as a function of field, temperature, molecule concentration and kind should yield information on the mechanisms involved in the exchange of charge between neighbouring localized sites (dopant molecules). Figure 17 shows the concentration dependence of the drift mobility for a number of molecularly doped systems. The exponential decrease of the mobility with increasing average intersite distance ρ is taken as evidence that transport indeed involves hopping. The slope γ of the $\log \mu$ versus ρ plot gives a measure of the decay of the wave function outside the transport active molecules. Hence, from the transit time data, information on a microscopic quantity is obtained !

Similar to hole transport in a-Se a transition from Gaussian to non-Gaussian transport is observed for hole transport in poly(*N*-vinylcarbazole), PVK. On the other hand, as shown in fig. 18 hole transport in brominated PVK, where the Br substitution occurs at the 3 or 6 position on the carbazole ring, remains dispersive over the entire experimental temperature range in a fashion similar to a-As_2Se_3 (Pfister and Griffiths 1978). Hence, PVK and 3Br–PVK constitute model systems for hopping transport which show features similar to the model chalcogenide glasses.

The different temperature behaviour of the dispersion in the two polymers might be connected to subtle differences in their morphology. Unsubstituted PVK undergoes ' crystallization ' to produce folded chain paracrystals (Griffiths

Fig. 17

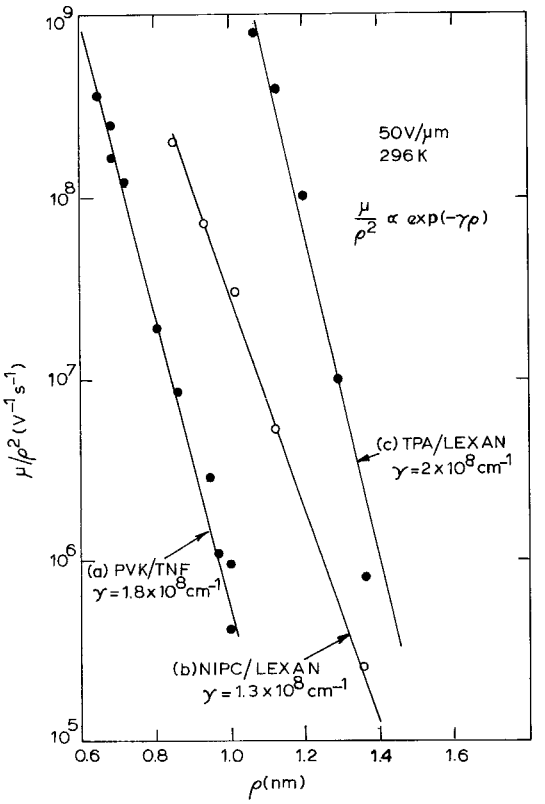

Dependence of drift mobility on distance between localized site for various organic disordered solids ((*a*) after Gill 1972, (*b*) Mort *et al.* 1976 and (*c*) Pfister 1977 a).

1975). In a projection down the chain axis of these crystals, the carbazole groups appear to have a regular trigonal symmetry about this axis. Although the interchain carbazole symmetry is lost in amorphous PVK, the intrachain carbazole symmetry and a considerable degree of chain parallelism are probably maintained. On the other hand, for the bromine-substituted PVK the chain parallelism characteristic of unsubstituted PVK is not present and the polymer does not crystallize (Griffiths *et al.* 1977). The random substitution of the bromine in either the 3 or 6 position (identical in the monomer but not in the polymer) can lead to random polarization of the carbazole group and random steric complications which override the van der Waals interactions that lead to chain parallelism in unbrominated PVK. This results in a considerably greater randomness in interchain carbazole–carbazole distances and orientations in 3Br–PVK and, furthermore, suggests a change in the intrachain carbazole symmetry and interactions. It is proposed that the different degree of ordering present in PVK and 3Br–PVK is reflected in the different temperature behaviour of the dispersion of carrier propagation. Specifically, the increased randomness among the bromine substituted carbazole groups might be the

origin of the large relatively temperature-independent dispersion of transit hole transport in this carbazole polymer.

Trap-controlled hopping (§ 2) is proposed as novel transport mechanism that should be observable in a wide range of disordered solids. Unambiguous

Fig. 18

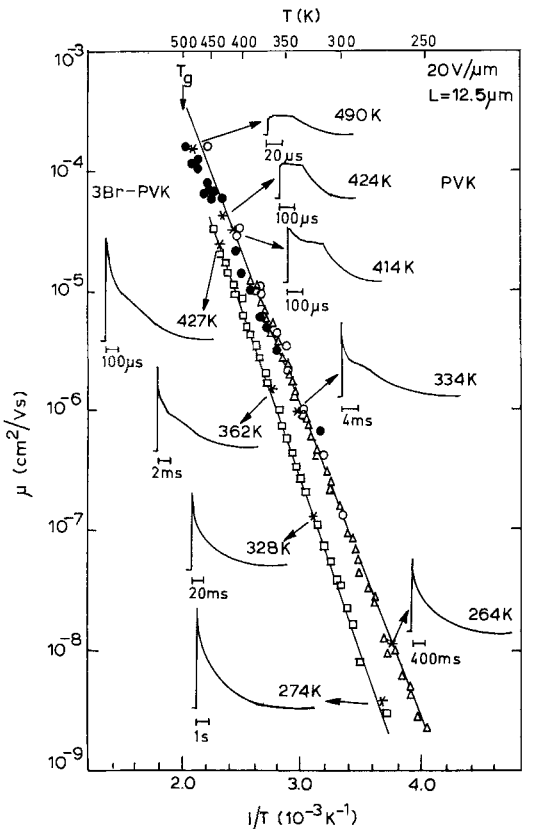

Temperature dependence of hole transport PVK and 3Br–PVK. Representative current traces are shown (after Pfister and Griffiths 1978).

evidence for this transport process has first been established for a molecularly doped polymers. In the specific example, hole transport in the solid solutions of polycarbonate, *N*-isopropyl carbazole (NIPC) and triphenylamine (TPA) was studied. Since the ionization potential of TPA is smaller than for NIPC, it was expected that TPA, at low concentrations, acts as a hole trap for holes hopping among the higher occupied molecular orbitals of the NIPC. Figure 19 summarizes the results of the time-of-flight experiments conducted at room temperature and with an applied field of 50 V/μm (Pfister *et al.* 1976). Plotted along the ordinate is the drift velocity L/t_T, where L is the sample thickness and t_T is the transit time determined from the logarithmic current-versus-time plots. It should be pointed out that at t_T about 10–15% of the injected carriers

transited the sample. Plotted along the abscissa is the TPA concentration, n_{TPA}, in units of molecules per cm^3. Concentrations were calculated from the weight ratio of dopant molecule to Lexan with 1·16 g/cm^3 as an average density.

Two sets of samples were measured. In one set the NIPC concentration was zero and the TPA concentration was varied. The hole velocities measured for these samples are shown as solid circles in fig. 19. With use of the same argument applied to establish hopping transport in NIPC-doped Lexan (Mort *et al.* 1976), the strong concentration dependence of L/t_T shown in fig. 19 also

Fig. 19

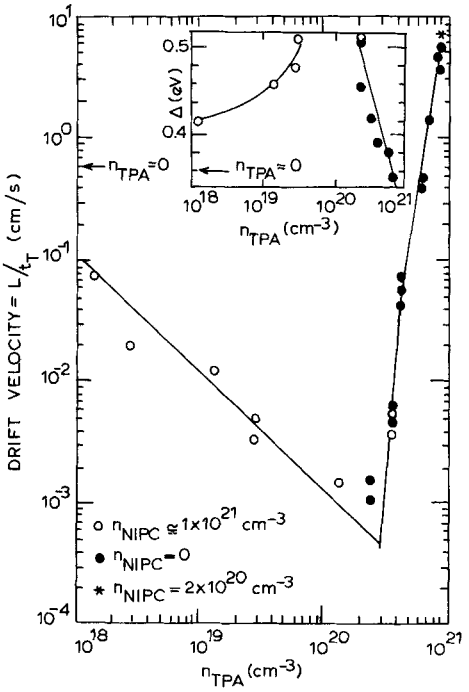

Plot of hole velocity L/t_T at 50 V/μm and 296 K as a function of triphenylamine, TPA (full circles) in Lexan polycarbonate. The open circles pertain to samples that contain, in addition to TPA, a fixed concentration of 1×10^{21} cm^{-3} *N*-isopropylcarbazole NIPC (after Pfister *et al.* 1976).

confirms this transport mechanism for the TPA/Lexan system. Thus at fixed temperature and field, the drift velocity is controlled by the overlap of the wave functions localized at neighbouring TPA molecules with average intersite distance $\rho_{TPA} \sim n_{TPA}^{-1/3}$.

In the other series of samples, Lexan was doped with NIPC molecules (with $n_{NIPC} = 1 \times 10^{21}$ cm^{-3}) and the TPA concentration was varied. n_{TPA} was kept below $\sim 3 \times 10^{20}$ cm^{-3} to ensure that the average intersite distance $\rho_{NIPC} \sim (n_{NIPC})^{-1/3}$ among the NIPC molecules was not changed by the TPA molecules. The drift-velocity results at 50 V/μm are shown in fig. 19 as the open circles. For $n_{TPA} = 0$ (arrow), transport occurs via hopping among NIPC

molecules. For the same concentration of $\sim 1 \times 10^{21}$ cm^{-3} transport via TPA molecules exceeds that via NIPC molecules by more than one order of magnitude.

The addition of TPA reduces the drift velocity from the value at $n_{\mathrm{TPA}} = 0$ in a manner which, for $n_{\mathrm{TPA}} \sim 10^{18}$–$10^{20}$ cm^{-3}, is approximately proportional to n_{TPA}^{-1}. With further increasing TPA concentration, the velocity goes through a minimum at $\sim 2 \times 10^{20}$ cm^{-3} and begins to rise again, approaching, at $\sim 3 \times 10^{20}$ cm^{-3}, the value obtained with films of the first sample series, which contained no NIPC. Samples with $n_{\mathrm{TPA}} > 4 \times 10^{20}$ cm^{-3} cannot be prepared without changing the average intersite distance among NIPC molecules. Also for total concentrations in excess of 2×10^{21} cm^{-3} crystallization effects became apparent.

From these concentration studies alone, it is possible to explain the general features of the observations in a relatively simple way. For $n_{\mathrm{TPA}} = 0$, the hole transport occurs via hopping among the NIPC molecules present in a fixed concentration. As TPA molecules are introduced at low concentrations, carriers occasionally become localized on a TPA molecule which, because its ionization potential is lower than NIPC, acts as a trap for holes. Since the overlap between TPA molecules is so small at these concentrations, further drift of the charge localized on TPA must await thermal excitation back to an NIPC molecule. The data points for $n_{\mathrm{TPA}} \lesssim 2 \times 10^{20}$ cm^{-3} pertain to this mechanism. At sufficiently high TPA concentrations, the overlap among the TPA molecules becomes sufficiently large that TPA–TPA hopping begins to compete with the hopping among NIPC–NIPC and TPA–NIPC pairs observed at low TPA loading. This process causes the drift velocity to rise for $n_{\mathrm{TPA}} \gtrsim 2 \times 10^{20}$ cm^{-3}; and it appears from the data shown in fig. 17 that at $n_{\mathrm{TPA}} \sim 4 \times 10^{20}$ hopping among TPA completely dominates the charge transport.

TPA in low concentrations inhibits hole transport through NIPC because its ionization potential is lower. It follows then that, in the converse case, charge transport through TPA should not be influenced by NIPC as long as the intersite distance $(n_{\mathrm{TPA}})^{-1/3}$ remains constant. This is experimentally confirmed in fig. 19 by the coincidence of the velocities measured for $n_{\mathrm{TPA}} \sim 4 \times 10^{20}$ cm^{-3} for both sample series and by the point identified by an asterisk which pertains to a sample with the loadings $n_{\mathrm{NIPC}} \sim 2 \times 10^{20}$ cm^{-3} and $n_{\mathrm{TPA}} \sim 8{\cdot}5 \times 10^{20}$ cm^{-3}.

These experiments clearly demonstrate the strength of the molecularly doped systems for the interpretation of transport data on a microscopic level. In chalcogenide glasses, the identification of transport mechanisms has to rely upon numerical arguments. For the organic systems, the ability to control the densities and species of the localized state produces unambiguous evidence for the underlying microscopic transport processes.

3.4.2. *a-SiO_2*

Transient hole transport in a-SiO_2 provides a further interesting example where non-dispersive and dispersive transport can be observed on the same sample. Unlike for a-Se or PVK where the transition between the two statistics occurs as a function of temperature and involves the same underlying transport mechanism, in a-SiO_2 the transition can be observed as a function of

time and involves two different transport processes, viz. the early time ' intrinsic ' and the late time ' extrinsic ' transport. Both these transport processes are believed to be hopping (Hughes 1977). In the experiments the charge carriers are generated in the bulk by an X-ray pulse of half width of ~ 3 ns. The electron mobility in a-SiO_2 is so high that they are swept out of the sample bulk within a few pico-seconds and therefore the current following the X-ray pulse at times $\gtrsim 5$ ns is due to hole motion (Hughes 1975, 1977). Following Hughes (1977), the holes created by ionizing radiation at a random site in the bulk of the SiO_2 film initially are transported by hopping among the $2p$ orbitals of neighbouring oxygen atoms. At these early times, the hole is expected to form a small polaron by distorting the lattice positions of nearby ions. The initial polaron hopping has been termed ' intrinsic ' transport process. The hole lifetime is of the order of 100 ns, after which it becomes trapped and proceeds its transport via hopping among structural defects (' extrinsic ' transport). The extrinsic process exhibits all the features of a non-Gaussian transport governed by a algebraic hopping time distribution function, eqn. (54), where $\alpha = \text{const}$. The dispersion depends upon the preparation of the oxide films and its corresponding α values range from $\sim 0{\cdot}14$ (McLean *et al.* 1975) to $\sim 0{\cdot}3$ (Hughes 1977).

The hole transport dispersion in a-SiO_2 is remarkably stable with temperature. Figure 20 shows a composite of transient voltage responses of a metal/SiO_2/Si MOS device (McLean *et al.* 1977). The composite recovery curve has been constructed from individual recovery traces measured at various temperatures. The individual traces were then shifted along the temperature axis by an amount calculated from the activation energy and the difference of experimental and reference temperature (297 K, top axis ; 87 K bottom axis). The solid line was calculated using the CTRW result for $\psi(t) \sim t^{-(1+\alpha)}$ where $\alpha = \text{const.} = 0{\cdot}22$

Fig. 20

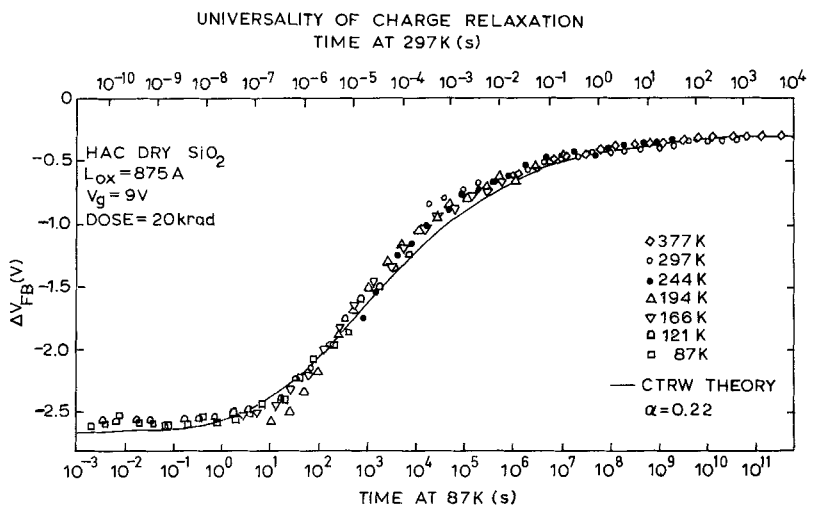

Master plot of voltage recovery of hole sweep out in metal/SiO_2/Si MOS devices. See § 3.4.2 (after McLean *et al.* 1975).

for the temperature range 87–377 K ! Note also the enormous time range over which the theoretical fit approximates the data (McLean *et al.* 1975).

The extrinsic hole mobility in a-SiO_2 is activated with $\sim 0{\cdot}37$ eV and the hopping site density is $\sim 10^{19}$ cm^{-3}. Interestingly, this value is of the same order as the hopping site density estimated for hole transport in a-As_2Se_3 (§ 4.3).

§ 4. Interpretation of transport mechanisms

4.1. *Introduction*

The theoretical concept of CTRW introduced in § 2.2 is generally applicable to any microscopic transport mechanism, whether hopping transport or transport in extended states. In fact, the mathematical equivalence between the formation of CTRW (Scher and Montroll 1975) and the generalized multiple-trapping formalism (Noolandi 1977, Schmidlin 1977) has been demonstrated in § 2.3. Hence, the analytical treatment of a specific transport mechanism will centre on the calculation of the event time distribution function $\psi(t)$ and specify its dependence on the microscopic transport parameters. Even if such a calculation were possible, the experimental verification of the assumed microscopic transport mechanism is exceedingly difficult and often ambiguous if the transit time dispersion and its temperature dependence are the only experimental inputs. This is the situation for amorphous chalcogenides, and the identification of the underlying mechanism of charge transport remains somewhat ambiguous. We believe that transport in these systems, a-Se and a-As_2Se_3, occurs via a hopping process and we provide the reasoning in the next paragraphs.

For doped organic polymers the situation is much clearer, since the kind and density of the transport states can be changed by materials preparation in a controlled and predictable manner. The dependence of the transit time upon the concentration of the dopant molecules clearly establishes hopping as underlying transport mechanism (fig. 17). Hence, these systems provide unique models for the study of dispersive and non-dispersive (fig. 18) hopping transport in disordered solids. Hopping in disordered systems is not synonymous with dispersive transport. The transition to non-dispersive transport at higher temperatures observed in PVK and the relative temperature insensitivity of the transit time dispersion in the related carbazole polymer 3Br–PVK (fig. 18) are clear evidence that the observation of a transit time dispersion depends on subtle differences in sample morphology, viz. the microscopic transport parameters.

4.2. *Doped polymers*

The key observable parameters of transport in doped polymers are γ, the empirical quantity describing the localization of the charge at the hopping site (fig. 17), and the activation energy Δ, the energy required to transfer the charge carrier between neighbouring localized sites. At room temperature and 50 V/μm applied field, these parameters have the typical values of $\gamma \sim 1\text{–}2 \times 10^8$ cm^{-1} and $\Delta \sim 0{\cdot}3\text{–}0{\cdot}6$ eV. No calculation of the overlap integral and activation energy associated with transfer of charge between localized sites is available for the doped organic system.

It is generally found that the overlap term, $\exp(-\gamma\rho)$, depends upon temperature and field (Pfister 1977 a) and that the activation energy depends on field (Gill 1972, Pfister 1977 a) and hopping distance (Pfister 1977 a). In dealing with these issues, one has to take into account that the picture of a charge transfer between localized sites is very simplified. In particular, positional disorder (hopping site distances) and a distribution of energy levels (activation energy) cannot obviously be separated. The hopping distance calculated from the dopant concentration assuming point-like molecules is indeed of the same order as the geometrical dimensions of the molecules themselves. Hence, the relative orientation of the molecules becomes an important factor for the transfer of the charge carrier, since the overlap term is extremely sensitive to the local morphology. A calculation of the overlap integral between the highest occupied molecular orbital of neighbouring NIPC molecules in vacuum shows that—as a function of the relative orientation at fixed distance between the centres of mass—this quantity varies by about seven orders of magnitude (Slowik and Chen 1977).

The strong dependence of the overlap on the relative orientation of neighbouring molecules may have some interesting consequences regarding the interpretation of the transport activation energy.

Given the fact that the overlap term can be maximized by relative rotational motion of neighbouring molecules, a carrier may await such an event before hopping to its neighbour. In such a case the electronic transport activation energy contains a term that describes the activation over rotational or librational barriers of pertinent groups of the dopant molecule. The observation of a temperature-dependent overlap term might indeed indicate that molecular motion plays an important role in electronic transport. The observation of trap-controlled hopping in mixed doped polymer systems (fig. 19) suggests that traps provide an additional source for the activation energy. Specifically, impurities with an ionization potential less than that of the dopant molecule may constitute traps for hole transport. Hence, the activation energy is expected to involve four terms, namely, Δ_p, Δ_d, Δ_t, Δ_r. Δ_p is the polaron binding energy which includes polarization of the polymer host matrix, Δ_d is the site-to-site fluctuation of the electronic transport levels, Δ_t is the energy difference between the transport levels of trapping molecules and hopping states and Δ_r is the activation energy for rotational or librational molecular motion.

The temperature dependence of the hole hopping mobility and transit time dispersion in poly(*N*-vinylcarbazole) is qualitatively very similar to that for hole transport in a-Se (figs. 9 and 18). Of particular interest is the observation of a transition from dispersive to non-dispersive transport as the temperature is raised which is not associated with a detectable change of the activation energy. Inspection of the current traces as a function of temperature shows that the hopping time distribution function $\psi(t)$ can be approximated by the power time dependence $t^{-(1+\alpha)}$, over a temperature range of ~ 315–355 K. At lower temperatures $\alpha_f < \alpha_i$ whereas at higher temperatures $\alpha_f > 1$ and $\alpha_i \rightarrow 1$ (Pfister and Griffiths 1978). With respect to PVK, the dispersion of hole transport for the bromine-substituted polymer, 3Br–PVK, is much less temperature sensitive and remains dispersive at the highest experimental temperature. In this case $\psi(t) \sim t^{-(1+\alpha)}$ is a good approximation in the temperature range

345–395 K. At lower temperatures $\alpha_f < \alpha_i$ and at higher temperatures $\alpha_f > 1$ and $\alpha_i \rightarrow 0{\cdot}8$ (Pfister and Griffiths 1978).

The data for hole hopping transport in PVK and 3Br–PVK thus demonstrate that the Scher–Montroll approximation of a hopping time distribution $\psi(t) \sim t^{(1+\alpha)}$ is a good approximation over some temperature range, but that more complicated $\psi(t)$'s are necessary to account for the data for all temperatures. The temperature dependence of the dispersion indicates that fluctuations of the various activation energies involved in charge transport (Δ_t, Δ_d, Δ_r) play an important role in the observed transit time dispersion. Finally, the different temperature dependence of the dispersion of hole hopping in the two closely related polymers demonstrates the subtle role played by sample morphology (§ 3.4).

4.3. *a-As_2Se_3*

The key features of transient hole transport in a-As_2Se_3 are its broad non-Gaussian dispersion which is strikingly temperature insensitive (fig. 4 (*a*)) and its high activation energy ($\sim 0{\cdot}6$ eV). Over the experimental temperatures and field range, the algebraic time dependence of $\psi(t)$ proposed by Scher and Montroll (1975), $\psi(t) \sim t^{-(1+\alpha)}$, provides a good consistent description for all experimental results.

The transport data for a-As_2Se_3 are best interpreted in terms of a trap-controlled hopping mechanism since, on the one hand, the constancy of the dispersion with respect to temperature cannot be reconciled with a multiple trapping model that has the trap depth as dominant random variable that produces all of the dispersion and, on the other hand, the activation energy is too large for conventional hopping transport. The analysis of hole transport in a-As_2Se_3 in terms of a generalized multiple-trapping model leads to the conclusion that both hopping and extended state motion are compatible with the experimental results but the most plausible view is (trap-controlled) hopping transport (Schmidlin 1977 b).

We propose that holes in a-As_2Se_3 hop through a density of localized transport states N_h, and achieve local thermal equilibrium with a trapping density $N_t \ll N_h$. The activation energy is associated with the hop from the trapping site (t) to the transport site (h) and the dispersion of the carrier packet is dominated by the randomness of the (t)–(h) site separation (which is the same as that of the (h)–(h) sites). It is likely that fluctuating trap energy levels also contribute to the transit time dispersion. A consistent interpretation of the numerics yields for a-As_2Se_3: $N_h \lesssim 10^{19}$ cm^{-3}, $N_t \gtrsim 10^{16}$ cm^{-3} (Pfister and Scher 1977 a).

The trapping states in the trap-controlled hopping process might be associated with the recently proposed ' intrinsic ' gap states in chalcogenide glasses (Mott *et al.* 1975, Kastner *et al.* 1976). It is argued that it is energetically favourable for the lowest energy neutral defects to pair-wise swap electrons, resulting in the reaction $2D \rightarrow D^+ + D^-$. This reaction is proposed to be exothermic due to strong electron–phonon coupling that is evident from the enormous Stokes shift of the photoluminescence (Street 1976). The charged defect states are spin-paired and hence could provide an explanation for the absence of E.S.R. in chalcogenide glasses. Kastner *et al.* (1976) described the formation of charged defects in terms of valence alternation. The lowest

energy defects, threefold coordinated chalcogen atoms (C_3^0), undergo a bond alternation to form a valence alternation pair in which one of the chalcogen atoms is singly coordinated negatively charged (C_1^-) and the other is threefold coordinated positively charged (C_3^+). These charged defect models have gone a long way to explaining luminescence (Street 1976, Street *et al.* 1974), non-radiative recombination and photoinduced structural changes (Street 1977) and photoinduced E.S.R. and midgap absorption (Bishop *et al.* 1975). Applying this model to the proposed trap-controlled hopping transport, one would predict that the holes hop through a set of localized states and interact with the higher lying D^- (or C_1^-) level. The occupation of the D^- level induces a rearrangement of the polarization of the environment of the trap which results in an upwards shift in energy to the D level. The net effect is that the carrier becomes trapped at the depth Δ_t of the D^- level but the reactivation into the transport states requires the additional energy such that the observed activation energy is composed of at least two terms $\Delta = \Delta_t + \Delta(D\text{–}D^-)$. An estimated upper limit of $\Delta(D\text{–}D^-)$ is $\sim 0{\cdot}3$ eV which yields $\Delta_t \sim 0{\cdot}3$ eV. This value for Δ_t is not unreasonable.

No correlation between electronic transport, photoinduced E.S.R. and absorption, all measurements that probe the density of gap states, has been reported to date. According to the Mott and Street model, such a correlation should exist since it associates the luminescence centre and the hole trap with the same defect D^- (or C_1^-). However, current measurements indicate that such a correlation is doubtful. By sample preparation techniques or doping, the drift mobility in a-As_2Se_3 can be changed by more than three orders of magnitude, but neither the intensity of the photoluminescence nor photoinduced E.S.R. changes in any correlated manner (Pfister and Taylor *et al.* 1978). For instance, alloying a-As_2Se_3 with AsI_3 (0·5 wt. % I) improves the hole mobility by at least a factor of 20, while alloying with 0·1 wt. % thallium reduces the mobility by more than two decades (Pfister *et al.* 1977, Pfister and Taylor *et al.* 1978). In both cases no change of the transport activation energy or transit time dispersion was observed. In terms of the proposed model, one would argue that iodine reduces and thallium enhances the negatively charged density, D^- (or C_1^-) as a result of charge compensation. That these density changes are not manifested in the spectroscopic measurements indicates either that the luminescence centre is not charged, as has been presumed (Street 1976) (or at least is not the D^-) or that the law of mass action cannot be applied in its proposed form. Certainly the defect chemistry of chalcogenide glasses is far from being understood and many more experiments on chemically modified glasses are necessary to obtain a more fundamental understanding of the gap states.

4.4. *a-Se*

The activation energy for hole transport in a-Se is $\sim 0{\cdot}27$ eV at 10 V/μm, which remains constant throughout the entire temperature range of the transition and down to at least ~ 120 K (fig. 9). It is possible that at temperatures higher than 240 K, a transition to a lower activation energy is indicated in the log L/t_T versus $1/T$ plot (fig. 9) but, due to the overall deviation from the Arrhenius temperature dependence in the neighbourhood of the glass transition, the experimental data cannot establish such a transition with certainty. The

observation of a transition from Gaussian to non-Gaussian transport at ~ 180 K and the strikingly well defined single activation energy below ~ 240 K poses some restrictions on the choice of microscopic transport models. Certainly conventional hopping with temperature-independent hopping density and fixed hopping energy can be ruled out. Also, one would expect that a multiple trapping model using a non-peaked density of gap states would contradict the observed constancy of the activation energy.

Apart from these minor limitations, all transport mechanisms discussed in § 2.4 are, in principle, compatible with the experimental results. A detailed computer analysis using the multiple-trap formulation showed that the entire temperature and thickness dependence of the hole current shape and transit time can be explained in terms of three traps with different but temperature-dependent capture cross-section and release rate (Noolandi 1977 a). Within experimental error, the depth of *all* three traps is $\sim 0{\cdot}3$ eV. Obviously, such a trap distribution needs some further physical justification. In any case, these results suggest that the distribution of release rates from the traps arises entirely from variations of the pre-exponential factor which strongly supports trap-controlled hopping as transport mechanism. Hence the prefactors of the release rates can be interpreted as representing the distribution of the overlap integrals (hopping site distances).

§ 5. Concluding remarks

There is unambiguous experimental evidence that, for a large number of disordered solids, transient electronic transport as observed in time-of-flight measurements reflects the existence of a significant fluctuation of microscopic event times. In fact, the results shown for transient hole transport in a-Se and carbazole polymers suggest that under appropriate experimental conditions, most likely determined by an upper value of the temperature, all disordered solids will exhibit a broad dispersion of carrier transit times. These features are independent of the transport mechanism and simply reflect the fact that the microscopic transport events are characterized by exponentials $\exp(x)$ where the random variable x (for instance Δ/kT, $\gamma\rho$) is much larger than unity, such that trivial fluctuations in x induce large fluctuations in the event times. The resulting event time distribution can be sufficiently broad that the experimental transit time becomes part of the distribution. Under these circumstances, the broadening of the propagating carrier packet—injected into the solid, for instance, by a pulse of strongly absorbed light—no longer can be described in terms of Gaussian statistical spreading.

On the experimental side, there appears little dispute that the time-of-flight current pulses exhibit features incompatible with a conventional statistical analysis that assumes Gaussian broadening of the carrier packet. There might be some disagreement about the actual pulse shapes observed in various samples, as has recently been pointed out by Godson and Hirsch (1977) for the case of electron transport in PVK : TNF, but we do not feel that such observations challenge the overall validity of the concept of non-Gaussian transport put forward in this review. It is well known that transient pulse shapes are distorted by the presence of surface traps and non-uniform fields, e.g. as shown

in Pfister and Scher (1977 a). Furthermore one has to bear in mind that the power law time dependence assumed for the event time distribution function $\psi(t)$ presents only one example of non-Gaussian transport. Other distribution functions leading to different time dependences of the transient current can be chosen to model non-Gaussian behaviour. The selected $\psi(t)$ represents an ideal case since the equations of a CTRW based on this distribution function can be analytically solved.

The observation of non-Gaussian transport itself does not specify the transport mechanism. While for the organic material transport undoubtedly occurs by hopping, the issue of whether holes in the inorganic solids proceed in extended states or in a hopping channel is not resolved and, until appropriate materials modification is available, can very likely not be solved to everybody's satisfaction. Indeed, models of extended state-transport have been proposed that explain the overall features of transient hole transport in chalcogenide glasses as well as does hopping transport (Fisher *et al.* 1976, Marshall 1977). We believe, however, that the values of the parameters obtained from these analyses are more compatible with hopping transport (Pfister and Scher 1977 a, Noolandi 1977 a, Schmidlin 1977 b).

The framework of CTRW was initially introduced to give a model for hopping transport and for simplicity of discussion and calculation. SM chose to deal with a fixed hopping energy in a random network. It is apparent that this framework is more general and can model any kind of transport mechanism. This has been conclusively demonstrated by the mathematical equivalence between the multiple-trapping formalism and CTRW (Schmidlin 1977 a, b, Noolandi 1977 b).

There is general agreement that any kind of transport in the presence of sufficiently fluctuating energy levels can give rise to non-Gaussian behaviour and that the associated distribution function is temperature dependent—as observed for holes in a-Se or PVK. However, the issue has recently been raised as to whether hopping transport through random sites but fixed activation energy is compatible with non-Gaussian statistics, implying that under these circumstances transport is always well defined (Pollak 1977, Silver 1977). Theoretically, the situation is unclear since an analytically satisfactory proof of these arguments has not been produced so far (cf. § 2.6). Experimentally one would look for a clearly defined hopping system which shows non-Gaussian transport with a temperature-independent dispersion—at least over a sufficiently wide temperature range that fluctuating energy levels can be safely excluded. However, this approach has been unsuccessful so far, since all systems undergo a transition to non-dispersive behaviour with increasing temperature. Hence for all known hopping systems, fluctuating energy levels have to be considered in the mathematical analysis. It is indeed suggested that, at least for disordered organic solids where the separation and spatial dimension of the hopping sites are comparable, disorder in hopping distance and activation energy cannot be separated.

In our opinion only the most global features of dispersive non-Gaussian transport have been covered by experiment and theory. The next improvements will have to deal with issues more microscopic in origin. Dispersive current shapes for well-defined systems that exhibit hopping or extended-state transport will have to be compared with experimental dependences predicted

from theories that are built on detailed microscopic models. Thus non-Gaussian transport is expected to remain an area of active interest which continues to offer a challenge to both theory and experimental work.

References

Abkowitz, M., and Pai, D. M., 1978, *Phys. Rev.* B, May 15.

Abkowitz, M., and Scharfe, M. E., 1977, *Solid St. Commun.*, **23,** 305.

Abkowitz, M., and Scher, H., 1977, *Phil. Mag.*, **35,** 1585.

Ambegoakar, V., Halperin, B. I., and Langer, J. S., 1971, *Phys. Rev.* B, **4,** 2612.

Apsley, N., and Hughes, H. P., 1975, *Phil. Mag.*, **30,** 963, 1327.

Bishop, S. G., Strom, U., and Taylor, P. C., 1975, *Phys. Rev. Letters*, **34,** 1346.

Dransfeld, K., and Hunklinger, S., 1977, *Proc. 7th Int. Conference on Amorphous and Liquid Semiconductors*, Edinburgh, edited by W. E. Spear, p. 155.

Fisher, F. D., Marshall, J. M., and Owen, A. E., 1976, *Phil. Mag.*, **33,** 261.

Funabashi, K., and Rao, B. N., 1976, *J. chem. Phys.*, **64,** 1561.

Gill, W. D., 1972, *J. appl. Phys.*, **43,** 5033.

Gill, W. D., 1974, *5th Int. Conference on Amorphous and Liquid Semiconductors*, Garmisch-Partenkirchen, 1973, edited by J. Stuke and W. Brenig (London : Taylor & Francis Ltd), p. 901.

Griffiths, C. H., 1976, *J. Polymer Sci.*, A2, **13,** 1167.

Griffiths, C. H., Okumura, K., and Vanlaeken, A., 1977, *J. Polymer Sci.*, A2, **15,** 1627.

Hughes, R. C., 1975, *Phys. Rev. Lett.*, **35,** 449 ; 1977, *Phys. Rev.* B, **15,** 2012.

Hurst, C. H., and Davis, E. A., 1974, *J. non-crystalline Solids*, **16,** 343.

Kastner, M., Adler, D., and Fritzsche, H., 1976, *Phys. Rev. Lett.*, **37,** 1304.

Kirkpatrick, S., 1973, *Rev. mod. Phys.*, **45,** 574.

Kolomiets, B. T., Lyubin, V. M., Nalivaiko, V. I., Formina, V. I., and Tsukerman, V. G., 1973, *Sov. Phys. Semicond.*, **6,** 1818.

Leal Ferreira, G. F., 1977, *Phys. Rev.* B, **16,** 4719.

Marshall, J. M., 1977, *Phil. Mag.*, **36,** 959.

Marshall, J. M., and Miller, G. R., 1973, *Phil. Mag.*, **27,** 1151.

Marshall, J. M., and Owen, A. E., 1971, *Phil. Mag.*, **24,** 1281.

McCrum, N. G., Read, B. E., and Williams, G., 1967, *Anelastic and Dielectric Effects in Polymeric Solids* (New York : John Wiley).

McLean, F. B., Boesch, H. E., Jr., and McGarrity, J. M., 1975, *I.E.E.E. Trans. nucl. Sci.*, **22,** 2163.

Montroll, E. W., and Scher, H., 1973, *J. Stat. Phys.*, **9,** 101.

Mort, J., and Pai, D. M. (editors), 1976, *Photoconductivity and Related Phenomena* (Elsevier).

Mort, J., Pfister, G., and Grammatica, S., 1976, *Solid St. Commun.*, **18,** 693.

Mott, N. F., 1977, *Contemp. Phys.*, **18,** 225.

Mott, N. F., Davis, E. A., and Street, R. A., 1975, *Phil. Mag.*, **32,** 961.

Noolandi, J., 1977 a, *Solid St. Commun.*, **24,** 477 ; 1977 b, *Phys. Rev.* B, **16,** 4466, 4474.

Owen, A. E., and Spear, W. E., 1976, *Physics Chem. Glasses*, **17,** 174.

Pfister, G., 1974, *Phys. Rev. Lett.*, **33,** 1474 ; 1976 a, *Ibid.*, **36,** 271 ; 1976 b, *Proc. 13th Int. Conference on Physics of Semiconductors*, Rome, edited by F. G. Fumi, p. 537 ; 1977 a, *Phys. Rev.* B, **16,** 3676 ; 1977 b, *Phil. Mag.*, **36,** 1147.

Pfister, G., Grammatica, S., and Mort, J., 1976, *Phys. Rev. Lett.*, **37,** 1360.

Pfister, G., and Griffiths, C. H., 1978, *Phys. Rev. Lett.*, **40,** 659.

Pfister, G., Melnyk, A. R., and Scharfe, M. E., 1977, *Solid State Commun.*, **21,** 907.

Pfister, G., and Scher, H., 1977 a, *Phys. Rev.* B, **15,** 2062 ; 1977 b, *Proc. 7th Int. Conference on Liquid and Amorphous Semiconductors*, Edinburgh, edited by W. E. Spear, p. 197.

Pfister, G., Liang, K., Morgan, M., Taylor, P. C., Friebele, E. J., and Bishop, S. G., 1978, *Phys. Rev. Lett.* (in the press).

Pollak, M., 1972, *J. non-crystalline Solids*, **11,** 1 ; 1977, *Phil. Mag.*, **36,** 1157.

PYKE, R., 1961, *Ann. math. statist.*, **32**, 1231, 1243.
SCHARFE, M., 1970, *Phys. Rev.* B, **2**, 5025.
SCHER, H., and LAX, M., 1973, *Phys. Rev.* B, **7**, 4491, 4502.
SCHER, H., and MONTROLL, E. W., 1975, *Phys. Rev.* B, **12**, 2455.
SCHER, H., MORT, J., and PAI, D. M., 1971, *J. appl. Phys.*, **42**, 3939.
SCHMIDLIN, F. W., 1977 a, *Solid St. Commun.*, **22**, 451 ; 1977 b, *Phys. Rev.* B, **16**, 2362.
SHLESINGER, M., 1974, *J. Stat. Phys.*, **10**, 421.
SILVER, M., 1977, *Eighth International Molecular Crystal Conference*, Santa Barbara.
SILVER, M., and COHEN, L., 1977, *Phys. Rev.* B, **15**, 3276.
SILVER, M., DY, K. S., and HUANG, I. L., 1971, *Phys. Rev. Lett.*, **27**, 21.
SLOWIK, J. H., 1977, *Bull. Am. phys. Soc.*, **22**, 434.
SPEAR, W. E., 1969, *J. non-crystalline Solids*, **1**, 197.
STREET, R. A., 1976, *Adv. Phys.*, **25**, 397 ; 1977, *Solid St. Commun.*, **24**, 365.
STREET, R. A., SEARLE, T. M., and AUSTIN, I. G., 1974, *Phil. Mag.*, **29**, 1157.
TUTIHASI, S., 1976, *J. appl. Phys.*, **47**, 277.
ZELLER, R. C., and POHL, R. O., 1971, *Phys. Rev.* B, **4**, 2029.
